

Dark matter in the $SO(5) \times U(1)$ gauge-Higgs unification

Shuichiro Funatsu*, Hisaki Hatanaka†, Yutaka Hosotani*

Yuta Orikasa†,‡ and Takuya Shimotani*

**Department of Physics, Osaka University, Toyonaka, Osaka 560-0043, Japan*

†School of Physics, KIAS, Seoul 130-722, Republic of Korea

and

‡Department of Physics and Astronomy, Seoul National University,

Seoul 151-742, Republic of Korea

Abstract

In the $SO(5) \times U(1)$ gauge-Higgs unification the lightest, neutral component of n_F $SO(5)$ -spinor fermions (dark fermions), which are relevant for having the observed unstable Higgs boson, becomes the dark matter of the universe. We show that the relic abundance of the dark matter determined by WMAP and Planck data is reproduced, below the bound placed by the direct detection experiment by LUX, by a model with one light and three heavier ($n_F = 4$) dark fermions with the lightest one of a mass from 2.3 TeV to 3.1 TeV. The corresponding Aharonov-Bohm phase θ_H in the fifth dimension ranges from 0.097 to 0.074. The case of $n_F = 3$ ($n_F = 5, 6$) dark fermions yields the relic abundance smaller (larger) than the observed limit.

1 Introduction

The Higgs boson of a mass around 125.5 GeV was discovered at LHC.[1, 2] It is not clear, however, whether or not the particle discovered is precisely the Higgs boson specified in the standard model (SM). Physics beyond the standard model may be hiding, showing up at the upgraded LHC. Couplings of the Higgs boson to other particles may slightly deviate from those in SM, and new particles may be produced, say, in the 4 - 7 TeV range. SM lacks a principle governing dynamics of the Higgs boson. Further SM has no clue to explain the dark matter (DM) in the universe.

In the gauge-Higgs unification (GHU) the Higgs boson is unified with gauge bosons. The 4D Higgs boson appears as a part of the extra-dimensional component of gauge fields so that its dynamics are governed by the gauge principle.[3]-[8] It has been shown that in the $SO(5) \times U(1)$ GHU in the Randall-Sundrum warped space the low energy physics appears almost the same as that in SM, consistent with all LHC data.[9]-[16] Contributions of Kaluza-Klein (KK) excited modes to the $H \rightarrow \gamma\gamma$ decay, for example, turn out very small.[15] Higgs couplings to gauge bosons, quarks and leptons at the tree level are suppressed by a common factor $\cos \theta_H$ where θ_H is the Aharonov-Bohm phase in the extra dimension.[17]-[22] All of the precision measurements, the tree-unitary constraint, and the Z' search indicate that $\theta_H < 0.2$. [9, 23] The $SO(5) \times U(1)$ GHU predicts new structure at higher energies. The masses of the 1st KK modes of Z and γ are predicted to be $3 \sim 7$ TeV for $\theta_H = 0.1 \sim 0.2$. The Higgs cubic and quartic self-coupling should be smaller than those in the SM by 10% - 20%.[16] Many other signals of GHU have been investigated.[24]-[33]

Another important issue is the dark matter.[34] Supersymmetric theory, the leading model of physics beyond the SM, predicts the lightest supersymmetric particle as a dark matter candidate.[35, 36] The lightest KK particle in universal extra dimension models [37]-[42], the lightest T-odd particle in the little Higgs models [43, 44], a fermionic composite state in the composite Higgs models [45]-[47], and axions [48]-[52] can be identified as dark matter. In the Higgs portal scenario the Higgs boson couples to dark matter in the hidden sector [53]-[57], and the dynamical dark matter scenario has been proposed.[58] Is there a dark matter candidate in the $SO(5) \times U(1)$ gauge-Higgs unification model? Can it explain the relic abundance reduced from the WMAP/Planck data and other observations, within the constraints from direct detection searches? A few scenarios for dark matter in GHU have been proposed.[59, 60, 61, 62] In this paper we would like to show that the realistic $SO(5) \times U(1)$ gauge-Higgs unification model contains a natural candidate for dark matter.

In the minimal $SO(5) \times U(1)$ gauge-Higgs unification model, in which only quark-lepton vector multiplets and associated brane fermions are introduced in the fermion sector, the effective potential is minimized at $\theta_H = \frac{1}{2}\pi$, which in turn implies that the Higgs boson becomes stable, contradicting with the observation.[11, 13, 61] To have an unstable Higgs boson, it is necessary to introduce fermion multiplets in the spinor representation of $SO(5)$ which do not appear at low energies.[15] Indeed, the presence of these fermions, with the gauge fields and top quark multiplet, naturally leads to $0 < \theta_H < \frac{1}{2}\pi$, yielding predictions consistent with the observation. One remarkable property is that independent of the details of these $SO(5)$ -spinor fermions there appears the universality relations among θ_H , the masses of KK Z /photon, and the Higgs self couplings.

We show that the lightest, neutral component of the $SO(5)$ -spinor fermions is absolutely stable, and becomes the dark matter of the universe. For this reason the $SO(5)$ -spinor fermion is called as a dark fermion in the present paper. It is heavy with a mass around $2 \sim 4$ TeV, but its couplings to the Higgs boson are small. From its relic abundance the number and structure of the dark fermion multiplets are inferred. It is curious that the Higgs dynamics are intimately related to the dark matter in the gauge-Higgs unification.

The paper is organized as follows. In Section 2 the $SO(5) \times U(1)$ model is introduced. In Section 3 it is shown that the neutral components of dark fermions become the dark matter, and the relic abundance is evaluated. In Section 4 the spin-independent cross section of the dark matter candidate with nucleons is evaluated, and the compatibility with the constraint coming from the direct detection experiments, XENON100 and LUX [63, 64], is examined. It will be found that the model with $n_F = 4$ nondegenerate dark fermions with the lightest one of a mass $2.3 \text{ TeV} \sim 3.1 \text{ TeV}$ explains the relic abundance of the dark matter determined from the WMAP/Planck data below the bound placed by the direct detection observation of LUX. Section 5 is devoted to the conclusion and discussions. In the appendices wave functions and couplings of dark fermions and relevant gauge bosons are summarized.

2 Model

The model of the $SO(5) \times U(1)$ GHU is defined in the Randall-Sundrum (RS) warped space with a metric

$$ds^2 = G_{MN} dx^M dx^N = e^{-2\sigma(y)} \eta_{\mu\nu} dx^\mu dx^\nu + dy^2, \quad (2.1)$$

where $\eta_{\mu\nu} = \text{diag}(-1, 1, 1, 1)$, $\sigma(y) = \sigma(y + 2L) = \sigma(-y)$, and $\sigma(y) = k|y|$ for $|y| \leq L$. The Planck and TeV branes are located at $y = 0$ and $y = L$, respectively. The bulk region $0 < y < L$ is anti-de Sitter (AdS) spacetime with a cosmological constant $\Lambda = -6k^2$. The warp factor $z_L \equiv e^{kL}$ is large, $z_L \gg 1$, and the Kaluza-Klein mass scale is given by $m_{KK} = \pi k/(z_L - 1) \sim \pi k z_L^{-1}$.

The model consists of $SO(5) \times U(1)_X$ gauge fields (A_M, B_M) , quark-lepton multiplets Ψ_a , $SO(5)$ -spinor fermions (dark fermions) Ψ_{F_i} , brane fermions $\hat{\chi}_{\alpha R}$, and brane scalar $\hat{\Phi}$. [12, 15] The bulk part of the action is given by

$$\begin{aligned}
S_{\text{bulk}} = \int d^5x \sqrt{-G} \Big[& -\text{tr} \left(\frac{1}{4} F^{(A)MN} F_{MN}^{(A)} + \frac{1}{2\xi} (f_{\text{gf}}^{(A)})^2 + \mathcal{L}_{\text{gh}}^{(A)} \right) \\
& - \left(\frac{1}{4} F^{(B)MN} F_{MN}^{(B)} + \frac{1}{2\xi} (f_{\text{gf}}^{(B)})^2 + \mathcal{L}_{\text{gh}}^{(B)} \right) \\
& + \sum_a \bar{\Psi}_a \mathcal{D}(c_a) \Psi_a + \sum_{i=1}^{n_F} \bar{\Psi}_{F_i} \mathcal{D}(c_{F_i}) \Psi_{F_i} \Big], \\
\mathcal{D}(c) = \Gamma^A e_A{}^M \Big(& \partial_M + \frac{1}{8} \omega_{MBC} [\Gamma^B, \Gamma^C] - ig_A A_M - ig_B Q_X B_M \Big) - c\sigma'(y). \quad (2.2)
\end{aligned}$$

The gauge fixing and ghost terms are denoted as functionals with subscripts gf and gh, respectively. $F_{MN}^{(A)} = \partial_M A_N - \partial_N A_M - ig_A [A_M, A_N]$, and $F_{MN}^{(B)} = \partial_M B_N - \partial_N B_M$. The color $SU(3)_C$ gluon fields and their interactions have been suppressed in the present paper. The $SO(5)$ gauge fields A_M are decomposed as

$$A_M = \sum_{a_L=1}^3 A_M^{a_L} T^{a_L} + \sum_{a_R=1}^3 A_M^{a_R} T^{a_R} + \sum_{\hat{a}=1}^4 A_M^{\hat{a}} T^{\hat{a}}, \quad (2.3)$$

where $T^{a_L, a_R} (a_L, a_R = 1, 2, 3)$ and $T^{\hat{a}} (\hat{a} = 1, 2, 3, 4)$ are the generators of $SO(4) \simeq SU(2)_L \times SU(2)_R$ and $SO(5)/SO(4)$, respectively.

In the fermion part $\bar{\Psi} = i\Psi^\dagger \Gamma^0$ and Γ^M matrices are given by

$$\begin{aligned}
\Gamma^\mu = \gamma^\mu = \begin{pmatrix} & \sigma^\mu \\ \bar{\sigma}^\mu & \end{pmatrix}, \quad \Gamma^5 = \gamma^5 = \begin{pmatrix} 1 & \\ & -1 \end{pmatrix}, \\
\sigma^\mu = (1, \vec{\sigma}), \quad \bar{\sigma}^\mu = (-1, \vec{\sigma}). \quad (2.4)
\end{aligned}$$

The quark-lepton multiplets Ψ_a are introduced in the vector representation of $SO(5)$. In contrast, n_F dark fermions Ψ_{F_i} are introduced in the spinor representation. The c term in Eq. (2.2) gives a bulk kink mass, where $\sigma'(y) = k\epsilon(y)$ is a periodic step function with a

magnitude k . The dimensionless parameter c plays an important role in controlling profiles of fermion wave functions.

The orbifold boundary conditions at $y_0 = 0$ and $y_1 = L$ are given by

$$\begin{aligned}
\begin{pmatrix} A_\mu \\ A_y \end{pmatrix} (x, y_j - y) &= P_{\text{vec}} \begin{pmatrix} A_\mu \\ -A_y \end{pmatrix} (x, y_j + y) P_{\text{vec}}^{-1}, \\
\begin{pmatrix} B_\mu \\ B_y \end{pmatrix} (x, y_j - y) &= \begin{pmatrix} B_\mu \\ -B_y \end{pmatrix} (x, y_j + y), \\
\Psi_a(x, y_j - y) &= P_{\text{vec}} \Gamma^5 \Psi_a(x, y_j + y), \\
\Psi_{F_i}(x, y_j - y) &= \eta_{F_i} (-1)^j P_{\text{sp}} \Gamma^5 \Psi_{F_i}(x, y_j + y), \quad \eta_{F_i} = \pm 1, \\
P_{\text{vec}} &= \text{diag}(-1, -1, -1, -1, +1), \quad P_{\text{sp}} = \text{diag}(+1, +1, -1, -1). \tag{2.5}
\end{aligned}$$

The $SO(5) \times U(1)_X$ symmetry is reduced to $SO(4) \times U(1)_X \simeq SU(2)_L \times SU(2)_R \times U(1)_X$ by the orbifold boundary conditions. Various orbifold boundary conditions fall into a finite number of equivalence classes of boundary conditions.[65, 66] The physical symmetry of the true vacuum in each equivalence class of boundary conditions is dynamically determined at the quantum level by the Hosotani mechanism. Recently dynamics for selecting boundary conditions have been proposed as well.[67] The Hosotani mechanism has been explored and established, not only in perturbation theory, but also on the lattice nonperturbatively.[68]

The brane action S_{brane} contains brane fermions $\hat{\chi}_{\alpha R}(x)$, brane scalar $\hat{\Phi}(x)$, $A_\mu(x, y = 0)$ and $\Psi_a(x, y = 0)$. It manifestly preserves gauge-invariance in $SO(4) \times U(1)_X$. $\hat{\Phi}$ develops non-vanishing expectation value $\langle \hat{\Phi} \rangle \gg m_{\text{KK}}$, which results in spontaneous breaking of $SO(4) \times U(1)_X$ into $SU(2)_L \times U(1)_Y$ and in making all exotic fermions heavy.

The 4D Higgs field, which is a bidoublet in $SU(2)_L \times SU(2)_R$, appears as a zero mode in the $SO(5)/SO(4)$ part of the fifth dimensional component of the vector potential $A_y^{\hat{a}}(x, y)$ with custodial symmetry.[9, 69, 70] Without loss of generality one can set $\langle A_y^{\hat{a}} \rangle \propto \delta^{a4}$ when the EW symmetry is spontaneously broken. The zero modes of $A_y^{\hat{a}}$ ($a = 1, 2, 3$) are absorbed by W and Z bosons. The 4D neutral Higgs field $H(x)$ is a fluctuation mode of the Wilson line phase θ_H which is an Aharonov-Bohm phase in the fifth dimension;

$$\begin{aligned}
A_y^{\hat{4}}(x, y) &= \{ \theta_H f_H + H(x) \} u_H(y) + \cdots, \\
\exp \left\{ \frac{i}{2} \theta_H \cdot 2\sqrt{2} T^{\hat{4}} \right\} &= \exp \left\{ i g_A \int_0^L dy \langle A_y \rangle \right\},
\end{aligned}$$

$$f_H = \frac{2}{g_A} \sqrt{\frac{k}{z_L^2 - 1}} = \frac{2}{g_w} \sqrt{\frac{k}{L(z_L^2 - 1)}}. \quad (2.6)$$

Here the wave function of the 4D Higgs boson is given by $u_H(y) = [2k/(z_L^2 - 1)]^{1/2} e^{2ky}$ for $0 \leq y \leq L$ and $u_H(-y) = u_H(y) = u_H(y + 2L)$. $g_w = g_A/\sqrt{L}$ is the dimensionless 4D $SU(2)_L$ coupling.

For each generation two vector multiplets Ψ_1 and Ψ_2 for quarks and two vector multiplets Ψ_3 and Ψ_4 for leptons are introduced. In contrast, the dark fermion Ψ_{F_i} belongs to the spinor representation of $SO(5)$, having four components

$$\Psi_{F_i} = \begin{pmatrix} \psi_{l1}^i \\ \psi_{l2}^i \\ \psi_{r1}^i \\ \psi_{r2}^i \end{pmatrix}. \quad (2.7)$$

ψ_l^i and ψ_r^i are $SU(2)_L$ and $SU(2)_R$ doublets, respectively. They mix with each other for $\theta_H \neq 0$. The electric charge is given by $Q_{\text{EM}} = T^{3L} + T^{3R} + Q_X$. We take $Q_X = \frac{1}{2}$ for Ψ_{F_i} so that it contains charge 1 and 0 components.

The KK decomposition of Ψ_{F_i} fields are summarized in Appendix B. With the boundary condition (2.5) $\Psi_{F_i}(x, z)$ does not have zero modes, and is expanded in the KK modes $F_i^{+(n)}(x)$ and $F_i^{0(n)}(x)$ ($n = 1, 2, 3, \dots$) as in (B.1). The mass spectrum is determined by (B.7). With $\eta_{F_i} = +1$ in the boundary condition for Ψ_{F_i} in (2.5) and for small θ_H the odd KK number modes $F_i^{+(n)}, F_i^{0(n)}$ (n : odd) are mostly $SU(2)_R$ doublets, containing $SU(2)_L$ components slightly. The even KK number modes $F_i^{+(n)}, F_i^{0(n)}$ (n : even) are mostly $SU(2)_L$ doublets. Consequently the first KK modes $F_i^{+(1)}, F_i^{0(1)}$ couple to the $SU(2)_L$ gauge bosons (W and Z) very weakly. On the other hand, with $\eta_{F_i} = -1$, $F_i^{+(n)}, F_i^{0(n)}$ (n : odd) are mostly $SU(2)_L$ doublets, and the first KK modes $F_i^{+(1)}, F_i^{0(1)}$ couple to W and Z with the standard weak coupling strengths.

The dark fermion number is conserved so that the lightest mode of the dark fermions becomes stable. At the tree level the first KK modes $F_i^{+(1)}$ and $F_i^{0(1)}$ are degenerate. Their mass is about 1.5 TeV to 4 TeV. The charged component $F_i^{+(1)}$ receives radiative corrections by photon and becomes heavier than the neutral component $F_i^{0(1)}$. Their mass difference is estimated to be about 20 GeV for a cutoff scale $\Lambda = 100$ TeV. $F_i^{+(1)}$ eventually decays into $F_i^{0(1)}$ and SM particles.

The lightest modes of $F_i^{0(1)}$'s are absolutely stable, and become DM of the universe. In the following discussions we denote $F_i^{0(1)}$ simply by F_i^0 . We shall see below that the

observed relic abundance of the DM and the bound from direct detection search of DM particles put severe constraint on the value of θ_H and the number and degeneracy of dark fermions.

3 Relic density

By considering annihilations and decays of dark fermions in the early universe, one can evaluate the relic density of the dark fermion. We mostly follow the arguments in Refs. [34], [37] and [71]. The Boltzmann equation for F_i^0 is given by

$$\begin{aligned} \frac{dn_{(F_i^0)}}{dt} = & -3Hn_{(F_i^0)} - \sum_{X,X'} [\langle \sigma(\bar{F}_i^0 F_i^0 \rightarrow XX')v \rangle (n_{(F_i^0)} n_{(\bar{F}_i^0)} - n_{(F_i^0)}^{\text{eq}} n_{(\bar{F}_i^0)}^{\text{eq}})] \\ & - \sum_{X,X'} \left[\langle \sigma(F_i^- F_i^0 \rightarrow XX')v \rangle (n_{(F_i^0)} n_{(F_i^-)} - n_{(F_i^0)}^{\text{eq}} n_{(F_i^-)}^{\text{eq}}) \right] \\ & - \sum_j \left[\langle \sigma(\bar{F}_i^0 F_i^0 \rightarrow F_j^+ F_j^-)v \rangle (n_{(F_i^0)} n_{(\bar{F}_i^0)} - n_{(F_i^0)}^{\text{eq}} n_{(\bar{F}_i^0)}^{\text{eq}}) \right] \\ & - \sum_{X,X'} \left\{ \langle \sigma(F_i^0 X \rightarrow F_i^+ X')v \rangle n_{(F_i^0)} n_{(X)} - \langle \sigma v(F_i^+ X' \rightarrow F_i^0 X) \rangle n_{(F_i^+)} n_{(X')} \right\}. \quad (3.1) \end{aligned}$$

Similar relations are obtained for \bar{F}_i^0 and F_i^\pm . Here H is the Hubble constant, $n_{(F)}$ denotes the number density of F , and X represents a SM field. The number density of F in the thermal equilibrium is given by $n_{(x)}^{\text{eq}} = g_x(m_x T/2\pi)^{3/2} \exp(-m_x/T)$ where g_x and m_x are the number of the degrees of freedom and mass of x , respectively. If F^\pm is heavier than F^0 , a term describing $F^+ \rightarrow F^0 f \bar{f}'$ decay should be added on the right-hand side of (3.1);

$$- \left(n_{(F_i^+)} - n_{(F_i^+)}^{\text{eq}} \right) \Gamma(F_i^+ \rightarrow F_i^0 f \bar{f}'), \quad (3.2)$$

where f, f' are fermions in the SM and Γ denotes a decay width.

The effective interactions relevant to annihilations of dark fermions are given by

$$\begin{aligned} \mathcal{L}_{\text{eff}} \supset & Z_\mu \left\{ \sum_{i=1}^{n_F} \bar{F}_i^0 \gamma^\mu \frac{g_w}{\cos \theta_W} (V_F + \gamma_5 A_F) F_i^0 + \sum_{i=1}^{n_F} \bar{F}_i^+ \gamma^\mu \frac{g_w}{\cos \theta_W} (V_{F+} + \gamma_5 A_{F+}) F_i^+ \right. \\ & \left. + \sum_f \bar{f} \gamma^\mu \frac{g_w}{\cos \theta_W} (v_f + \gamma_5 a_f) f \right\} \end{aligned}$$

$$\begin{aligned}
& + \sum_{V=Z^{(1)}, Z_R^{(1)}} V_\mu \left\{ \sum_{i=1}^{n_F} \bar{F}_i^0 \gamma^\mu g_w (V_F^{(V)} + \gamma_5 A_F^{(V)}) F_i^0 + \sum_{i=1}^{n_F} \bar{F}_i^+ \gamma^\mu g_w (V_{F+}^{(V)} + \gamma_5 A_{F+}^{(V)}) F_i^+ \right. \\
& \quad \left. + \sum_f \bar{f} \gamma^\mu g_w (v_f^{(V)} + \gamma_5 a_f^{(V)}) f \right\} \\
& + \sum_{V=\gamma, \gamma^{(1)}} V_\mu \left\{ \sum_{i=1}^{n_F} \bar{F}_i^+ \gamma^\mu e (V_{F+}^{(V)} + \gamma_5 A_{F+}^{(V)}) F_i^+ + \sum_f \bar{f} \gamma^\mu e (v_f^{(V)} + \gamma_5 a_f^{(V)}) f \right\} \\
& - H \sum_{i=1}^{n_F} Y_{F_i} (\bar{F}_i^0 F_i^0 + \bar{F}_i^+ F_i^+) - H \sum_f y_f \bar{f} f \\
& + \sum_{V=\gamma, \gamma^{(1)}, Z, Z^{(1)}, Z_R^{(1)}} i g_{VW+W-} (\eta^{\mu\rho} \eta^{\nu\sigma} - \eta^{\mu\sigma} \eta^{\nu\rho}) \\
& \quad \times \{ W_\rho^- V_\sigma \partial_\mu W_\nu^+ + V_\rho W_\sigma^+ \partial_\mu W_\nu^- + W_\rho^+ W_\sigma^- \partial_\mu V_\nu \}, \tag{3.3}
\end{aligned}$$

and by charged currents in Eq. (3.4). Here H denotes the Higgs boson, and f refers to a fermion in the SM (quarks, leptons and neutrinos).

For the decays (3.2) the corresponding interaction terms in the effective Lagrangian are

$$\begin{aligned}
\mathcal{L}_{\text{eff}} \supset & \sum_{V=W, W^{(1)}, W_R^{(1)}} V_\mu \frac{g_w}{\sqrt{2}} \left\{ \sum_{i=1}^{n_F} \bar{F}_i^0 \gamma^\mu (V_F^{(V)} + \gamma_5 A_F^{(V)}) F_i^+ \right. \\
& \left. + \sum_{\{f, f'\}} U_{ff'}^{(V)\text{CKM}} \bar{f}' \gamma^\mu (v_f^{(V)} + \gamma_5 a_f^{(V)}) f \right\} + (h.c.), \tag{3.4}
\end{aligned}$$

where f and f' refer to up-type quark (neutrino) and down-type quark (charged lepton), respectively. A CKM-like mixing matrix $U^{(V)\text{CKM}}$ is a unit matrix for leptons and is assumed to approximately coincide to the CKM-matrix for $V = W$. For the spinor fermion F , the right- and left-handed couplings $g_{FR/L}^V \equiv g_w (V_F^{(V)} \pm A_F^{(V)})/2$ are given in the Appendix C.2.2, and for the SM fermions the couplings can be found in Ref. [16]. In particular, W_R boson is found to have no couplings to the SM fermions.

3.1 Decays v.s. conversions of charged dark fermions

At the quantum level, masses of F^\pm and F^0 receive finite corrections δm_{F^+} and δm_{F^0} , respectively, and the degeneracy is lifted by one-loop corrections involving the photon and KK photons, which appear only in δm_{F^+} as depicted in Fig. 1. The mass difference between

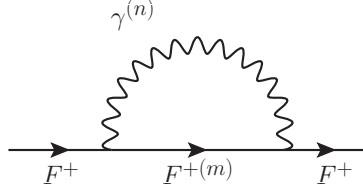


Figure 1: Diagrams contributing to the fermion mass difference $\Delta m_F = \delta m_{F^+} - \delta m_{F^0}$.

F^\pm and F^0 , $\delta m_{F^\pm} - \delta m_{F^0}$, can be evaluated in an analogous way as in the universal extra dimension [72], and in the case of the warped extra dimension it is estimated by

$$\delta m_{F^\pm} - \delta m_{F^0} \sim m_F \frac{\alpha_{\text{EM}}}{4\pi} \cdot K, \quad (3.5)$$

where α_{EM} is the electromagnetic fine-structure constant. In UED $K = \ln(\Lambda^2/\mu^2)$ where Λ and μ is the cut-off scale and a renormalization scale, respectively, and $\Lambda/\mu \sim \mathcal{O}(10)$. In the RS space-time only the first few KK excited states of each fields enter the quantum corrections. In particular the coupling of right-handed $F^{\pm(1)}$ to $\gamma^{(1)}$ is several times as large as the electromagnetic coupling. It follows that $K \sim \mathcal{O}(10)$. Similarly, quantum corrections due to higher-KK modes to the gauge couplings also become small, and a large cut-off scale is allowed.[73]

A charged dark fermion decays to a neutral dark fermion and a charged vector bosons, hence to charged leptons and neutrinos, or light down-type quarks and up-type antiquarks. (See Fig. 2)

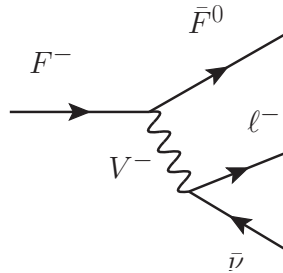


Figure 2: Charged dark fermion decay. ℓ^- and $\bar{\nu}$ can be replaced with down-type quarks and up-type anti-quarks, respectively.

In the $SO(5) \times U(1)$ GHU model, we have three charged vector bosons at low energies: W , the 1st KK excited state of W , and the lowest KK mode of the W_R boson. A charged dark fermion F^+ decays to F^0 mainly by emitting a W boson, because $W^{(1)}$ is heavy and interacts with F^+ and F^0 very weakly, and $W_R^{(1)}$ cannot decay to the SM fermions. If the

mass difference between the charged and neutral dark fermions, $\Delta m_F \equiv m_{F^\pm} - m_{F^0} \simeq \delta m_{F^\pm} - \delta m_{F^0}$, is much smaller than m_W , the decay rate is given by

$$\begin{aligned} \Gamma(F^- \rightarrow \bar{F}^0 \ell \bar{\nu}) &= \frac{G_F^2}{192\pi^3} m_{F^-}^5 [(g_{\ell\nu L}^{'W})^2 + (g_{\ell\nu R}^{'W})^2] \left\{ [(g_{FL}^{'W})^2 + (g_{FR}^{'W})^2] f\left(\frac{m_{F^0}^2}{m_{F^-}^2}\right) - 4g_{FL}^{'W}g_{FR}^{'W}g\left(\frac{m_{F^0}^2}{m_{F^-}^2}\right) \right\} \\ &= \frac{G_F^2}{192\pi^3} \Delta m_F^5 [(g_{\ell\nu L}^{'W})^2 + (g_{\ell\nu R}^{'W})^2] \left\{ \frac{64}{5} [(g_{FL}^{'W})^2 + (g_{FR}^{'W})^2 - g_{FL}^{'W}g_{FR}^{'W}] + \mathcal{O}\left(\frac{\Delta m_F^6}{m_F^6}\right) \right\}, \end{aligned} \quad (3.6)$$

where $g_{\ell\nu L/R}^{'V} \equiv g_{\ell\nu L/R}^V/g_w$, $g_{FL/R}^{'V} \equiv g_{FL/R}^V/g_w$ and

$$\begin{aligned} f(x) &= 1 - 8x + 8x^3 - x^4 - 12x^2 \ln x, \\ g(x) &= 1 + 9x - 9x^2 - x^3 + 6x(1+x) \ln x. \end{aligned} \quad (3.7)$$

In the second equality in (3.6), we have assumed $\Delta m_F \ll m_{F^\pm}, m_{F^0}$ and have invoked approximations

$$f((1-x)^2) = \frac{64}{5}x^5 - \frac{96}{5}x^6 + \mathcal{O}(x^7), \quad g((1-x)^2) = \frac{16}{5}x^5 - \frac{8}{5}x^6 + \mathcal{O}(x^7). \quad (3.8)$$

Hence the lifetime of F^- is given by

$$\tau_{F^\pm} \simeq \tau_\mu \left(\frac{m_\mu}{\Delta m_F} \right)^5 \frac{5}{64} [(g_{FL}^{'W})^2 + (g_{FR}^{'W})^2 - g_{FL}^{'W}g_{FR}^{'W}]^{-1}, \quad (3.9)$$

where $\tau_\mu = 2.2 \times 10^{-6}$ sec and $m_\mu = 105$ MeV are the lifetime and mass of the muon, respectively. $(g_{W\ell\nu}^{'L}, g_{W\ell\nu}^{'R}) = (1, 0)$ is used. In order that the F^\pm lifetime is much shorter than the typical time scale of the weakly interacting massive particle (WIMP)-DM formation, i.e. $\tau_{F^\pm} \ll 10^{-10}$ sec, the mass difference of dark fermions must be the order of 10 GeV or larger. The mass difference (3.5) will satisfy this condition for $m_F \gtrsim 2$ TeV with $K \sim \mathcal{O}(10)$. Hereafter we assume that these conditions are satisfied and F^\pm decays sufficiently quickly. We also note that if charged fermions F^\pm do not decay sufficiently fast, they would remain after the DM freeze-out and would subsequently decay to F^0 , resulting in doubling the relic DM density.

In the right-hand side of the Boltzmann equation (3.1), the last two terms correspond to $F^0 \leftrightarrow F^\pm$ conversion depicted in Fig. 3.

The process depicted as (A) in Fig. 3, in particular $F^+ F^-$ pair production through this process is kinematically allowed since $m_F \gg \Delta m_F$. Although the process depicted as (B) in Fig. 3 is suppressed by the small $F\bar{F}W$ coupling which is order of 10^{-3} , this conversion

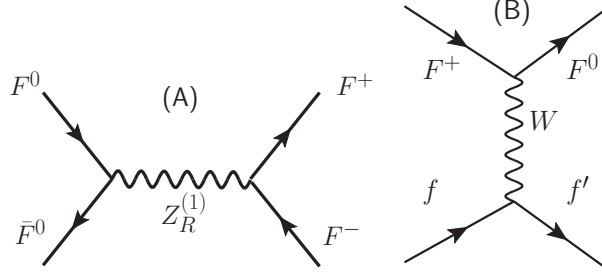


Figure 3: Processes of $F^0 \leftrightarrow F^+$ conversions. (A) $F^0 + \bar{F}^0 \leftrightarrow F^+ + F^-$ mediated by $Z_R^{(1)}$. (B) $F^0 + f \leftrightarrow F^+ + f'$ by exchanging the W boson, where f and f' are SM fermions.

process can dominate due to the large ratio of $n_{(X)}^{\text{eq}}/n_{(F)}^{\text{eq}} \sim (T/m_F)^{3/2} \exp(m_F/T) \sim 10^{10}$ for $T/m_F \sim 30$ [71].

Thus we have $n_{(F^\pm)}^{\text{eq}} \sim n_{(F^0)}^{\text{eq}}$ before the freeze-out, and after the freeze-out F^+ decay to F^0 . The relic density of the dark fermion in the present universe is given by the sum of the charged and neutral dark fermions at the freeze-out. In the followings we calculate the number density of all dark fermions.

3.2 Pair annihilations and relic density of dark fermions

The annihilation processes and corresponding diagrams of the dark fermions are tabulated in Table. 1 and Fig. 4. We note that the masses of the first excited states of SM fermions [bosons] are about m_{KK} [$0.8m_{KK}$]. Mass of dark fermions is smaller than the half of m_{KK} , so that the the final states of the annihilation of dark fermions involve only SM particles.

We consider the case where θ_H is small ($z_L \lesssim 10^5$ or $\theta_H \lesssim 0.15$). In such a case, dark fermion is heavy and some of annihilation amplitudes are processes are suppressed by $\sin^2 \theta_H$. We find that for most of the processes annihilation cross-sections are too small to explain the current relic density. In particular, we find that $\bar{F}FW$, $\bar{F}FZ$, $\bar{F}FZ^{(n)}$ and $Z_R^{(n)}WW$ couplings are suppressed by $\sin^2 \theta_H$ factor. (See Appendix C and D). One finds that the process (a-i) is suppressed by the small Higgs Yukawa couplings of $F\bar{F}$ and processes (a-ii) with $V = Z$ and $Z^{(n)}$ are suppressed by the small $Z^{(n)}F\bar{F}$ couplings. The processes (a-iii) and (a-iv) are suppressed by the small $W^-F^+\bar{F}$ and $ZF\bar{F}$ couplings. All processes of (a-v) are suppressed by the small $Z^{(n)}F\bar{F}$ coupling and small $Z_R^{(n)}W^+W^-$ couplings. Thus one finds that only the process (a-ii) with $V = Z_R^{(1)}$ is unsuppressed and could be enhanced by both the Breit-Wigner resonance[40] of $Z_R^{(1)}$ and the large right-handed couplings of $Z_R^{(1)}$ to quarks and leptons.

Table 1: Pair annihilation processes of dark fermions ($F = F^0, F^+$). (a-i)-(a-v) are annihilation processes of neutral and charged dark fermions, whereas (ac-i)-(ac-iv) are those of charged dark fermions. (co-i)-(co-v) are for co-annihilation of the neutral and charged dark fermions. In the intermediate states ‘ n ’ denotes the KK-excitation level ($n \neq 0$). In the final states q, l and ν denotes quarks, charged leptons and neutrinos in the SM. Corresponding diagrams are shown in Fig. 4.

	process	diagrams
annihilation		
(a-i)	$F\bar{F} \rightarrow (S = H, H^{(n)}) \rightarrow q\bar{q}, l\bar{l}$	(a)
(a-ii)	$F\bar{F} \rightarrow (V = Z, Z^{(n)}, Z_R^{(n)}) \rightarrow q\bar{q}, l\bar{l}, \nu\bar{\nu}$	(b)
(a-iii)	$F\bar{F} \rightarrow ZZ, t\text{- and }u\text{- channels}$	(c), (d)
(a-iv)	$F\bar{F} \rightarrow W^+W^-$ t-channel	(c)
(a-v)	$F\bar{F} \rightarrow (V = Z, Z^{(n)}, Z_R^{(n)}) \rightarrow W^+W^-$	(e)
(ac-i)	$F^+F^- \rightarrow \gamma\gamma, t\text{- and }u\text{-channels}$	(c) (d)
(ac-ii)	$F^+F^- \rightarrow Z\gamma, t\text{- and }u\text{-channels}$	(c) (d)
(ac-iii)	$F^+F^- \rightarrow (V = \gamma, \gamma^{(n)}) \rightarrow q\bar{q}, l\bar{l}$	(b)
(ac-iv)	$F^+F^- \rightarrow (V = \gamma, \gamma^{(n)}) \rightarrow W^+W^-$	(e)
co-annihilation		
(co-i)	$F^+\bar{F}^0 \rightarrow (V = W^+, W^{+(n)}, W_R^{+(n)}) \rightarrow q\bar{q}', \nu\bar{l}$	(b)
(co-ii)	$F^+\bar{F}^0 \rightarrow (V = W^+, W^{+(n)}, W_R^{+(n)}) \rightarrow W^+Z$	(e)
(co-iii)	$F^+\bar{F}^0 \rightarrow (V = W^+, W^{+(n)}, W_R^{+(n)}) \rightarrow W^+\gamma$	(e)
(co-iv)	$F^+\bar{F}^0 \rightarrow W^+Z, t\text{- and }u\text{-channels}$	(c), (d)
(co-v)	$F^+\bar{F}^0 \rightarrow W^+\gamma, t\text{- and }u\text{-channels}$	(c), (d)

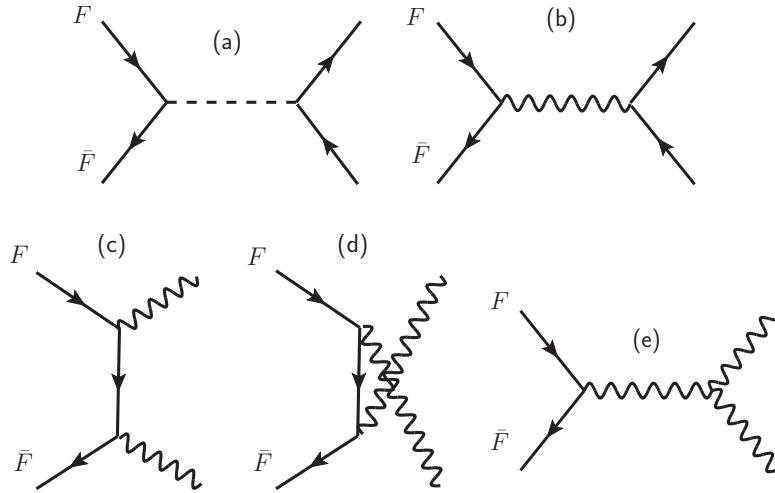


Figure 4: $F\bar{F}$ annihilation diagrams. (a) s-channel annihilation to a fermion-pair through the Higgs boson (b) s-channel, to fermions through a vector boson (c)(d) t- and u-channel annihilations to two vector bosons (e) s-channel annihilation to two vector bosons

For the annihilation of charged dark fermions, we see that the process (ac-i) is not suppressed by couplings. However, the annihilation cross section

$$\sigma(F_i^+ F_i^- \rightarrow \gamma\gamma) \cdot v = \frac{e^4}{8\pi m_F^2} + \mathcal{O}(v^2), \quad (3.10)$$

where v is the relative velocity of initial particles, is numerically small and negligible with $m_F \gtrsim 2 \text{ TeV}$. The process (ac-ii) is suppressed by $F\bar{F}Z$ couplings. The cross section in the process (ac-iii) with $V = \gamma$ is estimated as

$$\sum_f \sigma(F_i^+ F_i^- \rightarrow \gamma \rightarrow f\bar{f}) \cdot v = 8 \cdot \frac{e^4}{16\pi m_F^2} + \mathcal{O}(v^2). \quad (3.11)$$

The process (ac-iii) with $V = \gamma^{(1)}$ can be enhanced by both large right-handed coupling of fermions and Breit-Wigner resonances. The process (ac-iv) is suppressed by the small $\gamma^{(1)}W^+W^-$ coupling.

As for coannihilation, we have tabulated possible processes in Table. 1. We find that the process (co-i) with $V = W^+, W^{+(n)}$ is suppressed by small $F^+\bar{F}^0W^-$ couplings and the process (co-i) with $V = W_R$ is forbidden because of vanishing $W_R\bar{f}f$ couplings. The process (co-ii) with $V = W, W^{(n)}$ is suppressed by small $\bar{F}FW$ couplings, and (co-ii) with $V = W_R$ is suppressed by the small $W_R - W - Z$ couplings. The process (co-iii) with $V = W, W^{+(n)}$ is suppressed by small $F\bar{F}W^{(n)}$ couplings. The process (co-iii) with $V = W_R$ is forbidden by the vanishing $W_RW\gamma$ coupling which ensures the ortho-normality of the KK gauge bosons. The processes (co-iv) and (co-v) are suppressed by small $F\bar{F}Z$ and $F^+\bar{F}^0W^-$ couplings. Hence we found that all of the co-annihilation processes are either vanishing or strongly suppressed.

Thus we find that relevant processes for dark fermion annihilation are the following s-channel processes

$$\begin{aligned} F^0\bar{F}^0 &\rightarrow Z_R^{(1)} \rightarrow q\bar{q}, l\bar{l}, \nu\bar{\nu}, \\ F^+F^- &\rightarrow \gamma, \gamma^{(1)} \rightarrow q\bar{q}, l\bar{l}, \\ F^+F^- &\rightarrow Z_R^{(1)} \rightarrow q\bar{q}, l\bar{l}, \nu\bar{\nu}, \end{aligned} \quad (3.12)$$

and all other annihilation and co-annihilation processes are negligible.

In the followings, we calculate the relic density of the dark fermions using annihilation cross sections of the processes given in (3.12). For charged dark fermions, the annihilation cross section of $F_i^+ F_i^-$ to the SM fermions is given by

$$\begin{aligned} &\sum_f \sigma(F_i^+ F_i^- \rightarrow \{\gamma, \gamma^{(1)}, Z_R^{(1)}\} \rightarrow \bar{f}f) \\ &= 8 \cdot \frac{e^4}{16\pi\beta s^2} \left(s + 4m_F^2 + \frac{1}{3}s\beta^2 \right) \end{aligned}$$

$$\begin{aligned}
& + \frac{1}{64\pi\beta} \left[\frac{s}{(s - m_{Z_R^{(1)}}^2)^2 + m_{Z_R^{(1)}}^2 \Gamma_{Z_R^{(1)}}^2} g_w^4 \left(\sum_f \left[\left(g_{fL}^{Z_R^{(1)}} \right)^2 + \left(g_{fR}^{Z_R^{(1)}} \right)^2 \right] \right) \right. \\
& \quad \times \left\{ \left(1 + \frac{\beta^2}{3} \right) \left[\left(g_{F+L}^{Z_R^{(1)}} \right)^2 + \left(g_{F+R}^{Z_R^{(1)}} \right)^2 \right] + 8 \frac{m_F^2}{s} g_{F+L}^{Z_R^{(1)}} g_{F+R}^{Z_R^{(1)}} \right\} \\
& + \frac{s}{(s - m_{\gamma^{(1)}}^2)^2 + m_{\gamma^{(1)}}^2 \Gamma_{\gamma^{(1)}}^2} e^4 \left(\sum_f \left[\left(g_{fL}^{\gamma^{(1)}} \right)^2 + \left(g_{fR}^{\gamma^{(1)}} \right)^2 \right] \right) \\
& \quad \times \left\{ \left(1 + \frac{\beta^2}{3} \right) \left[\left(g_{F+L}^{\gamma^{(1)}} \right)^2 + \left(g_{F+R}^{\gamma^{(1)}} \right)^2 \right] + 8 \frac{m_F^2}{s} g_{F+L}^{\gamma^{(1)}} g_{F+R}^{\gamma^{(1)}} \right\} \\
& + 2 \cdot \frac{(s - m_{Z_R^{(1)}}^2)(s - m_{\gamma^{(1)}}^2) + m_{Z_R^{(1)}} m_{\gamma^{(1)}} \Gamma_{Z_R^{(1)}} \Gamma_{\gamma^{(1)}}}{[(s - m_{Z_R^{(1)}}^2)^2 + m_{Z_R^{(1)}}^2 \Gamma_{Z_R^{(1)}}^2][(s - m_{\gamma^{(1)}}^2)^2 + m_{\gamma^{(1)}}^2 \Gamma_{\gamma^{(1)}}^2]} \cdot s \\
& \quad \times g_w^2 e^2 \left(\sum_f \left[g_{fL}^{Z_R^{(1)}} g_{fL}^{\gamma^{(1)}} + g_{fR}^{Z_R^{(1)}} g_{fR}^{\gamma^{(1)}} \right] \right) \\
& \quad \times \left\{ \left(1 + \frac{\beta^2}{3} \right) \left[g_{F+L}^{Z_R^{(1)}} g_{F+L}^{\gamma^{(1)}} + g_{F+R}^{Z_R^{(1)}} g_{F+R}^{\gamma^{(1)}} \right] + 4 \frac{m_F^2}{s} \left[g_{F+L}^{Z_R^{(1)}} g_{F+R}^{\gamma^{(1)}} + g_{F+L}^{\gamma^{(1)}} g_{F+R}^{Z_R^{(1)}} \right] \right\}, \tag{3.13}
\end{aligned}$$

where $g_{FL/FR}^V \equiv V_F^{(V)} \mp A_F^{(V)}$, $g_{fL/fR}^V \equiv v_f^{(V)} \mp a_f^{(V)}$ ($V = Z_R^{(1)}, \gamma^{(1)}$) and the couplings are summarized in Sec. C.2. $\beta \equiv \sqrt{1 - 4m_F^2/s}$ and s is the invariant mass of $F\bar{F}$. We have neglected γ - $\gamma^{(1)}$ and γ - $Z_R^{(1)}$ interference terms. $F_i^0 \bar{F}_i^0$ annihilation cross section $\sum_f \sigma(F^0 \bar{F}^0 \rightarrow Z_R^{(1)} \rightarrow \bar{f}f)$ is obtained from (3.13) by replacing $f_{L/R+}^{(V)}$ with $f_{L/R}^{(V)} \equiv V_F^{(V)} \pm A_F^{(V)}$ and ignoring e^2 and e^4 terms. $\Gamma_{Z_R^{(1)}}$ and $\Gamma_{\gamma^{(1)}}$ are the total decay rate of $Z_R^{(1)}$ and $\gamma^{(1)}$ bosons, and $\Gamma_{Z_R^{(1)}}$ is estimated to be

$$\begin{aligned}
\Gamma_{Z_R^{(1)}} &= \sum_f N_{c,f} \frac{m_{Z_R^{(1)}}}{24\pi} g_w^2 \gamma \left(g_{fL}^{Z_R^{(1)}}, g_{fR}^{Z_R^{(1)}}, m_f^2/m_{Z_R^{(1)}}^2 \right) \\
&+ \sum_F \frac{m_{Z_R^{(1)}}}{24\pi} g_w^2 \left[\gamma \left(g_{F^0L}^{Z_R^{(1)}}, g_{F^0R}^{Z_R^{(1)}}, m_F^2/m_{Z_R^{(1)}}^2 \right) + \gamma \left(g_{F+L}^{Z_R^{(1)}}, g_{F+R}^{Z_R^{(1)}}, m_F^2/m_{Z_R^{(1)}}^2 \right) \right], \\
\gamma(g_L, g_R, x) &\equiv \sqrt{1 - 4x} [g_L^2 + g_R^2 - x(g_L^2 + g_R^2 - 6g_L g_R)]. \tag{3.14}
\end{aligned}$$

$\Gamma_{\gamma^{(1)}}$ is obtained in an analogous way. Here $N_{c,f} = 3$ (1) when f is a quark (charged lepton or neutrino). m_f is the mass of the SM fermion. We note that the F^\pm contributions in (3.14) are rather large.

Let n_0 [n_+] be the number-density of F_i^0 and \bar{F}_i^0 [F_i^+ and F_i^-] ($i = 1, \dots, n_F$), and σ_0 [σ_+] be the annihilation cross section of F_i^0 [F_i^+]. Then the evolution of the total number density of the DM, is given by $n \equiv 2n_F(n_0 + n_+)$, and the time-evolution of n is governed by the Boltzmann equation

$$\frac{dn}{dt} = -3Hn - 2n_F\langle\sigma_0 v\rangle(n_0^2 - n_{0,\text{eq}}^2) - 2n_F\langle\sigma_+ v\rangle(n_+^2 - n_{+,\text{eq}}^2), \quad (3.15)$$

where $n_{0/+,\text{eq}}$ is the number-density in the thermal equilibrium and approximated by $n_{0/+,\text{eq}} \approx g_{0/+}(m_{F^{0/\pm}}T/2\pi)^{3/2}\exp(-m_{F^{0/\pm}}/T)$ with $g_{0/+} = 2$ being the number of degrees of freedom of F_i^0 and F_i^+ . Using the relations $n_{0,+}/n_{0,+,\text{eq}} = n/n_{\text{eq}}$ and $n_{0,\text{eq}}/n_{\text{eq}} = n_{+,\text{eq}}/n_{\text{eq}} = 1/4n_F$, we obtain

$$\frac{dn}{dt} = -3Hn - \langle\sigma_{\text{eff}} v\rangle(n^2 - n_{\text{eq}}^2), \quad \sigma_{\text{eff}} v \equiv \frac{\sigma_0 v + \sigma_+ v}{8n_F}. \quad (3.16)$$

We introduce $Y_{(\text{eq})} \equiv n_{(\text{eq})}/S$ where $S = 2\pi^2 g_* T^3/45$ is the entropy density. g_* is the degree of freedom at the freeze-out temperature T_f and we take $g_* = 92$. Conservation of entropy per co-moving volume, $Sa_{sf}^3 = \text{constant}$ (a_{sf} is the scale factor of the expanding universe), reads $dn/dt + 3Hn = SdY/dt$. The Hubble constant is given by $H^2 = 4\pi^3 g_* T^4/(45M_{Pl}^2)$ and $t = 1/2H$ in the radiation-dominant era. M_{Pl} is the Planck mass. Hence we rewrite the Boltzmann equation as

$$\frac{dY}{dx} = \frac{\langle\sigma_{\text{eff}} v\rangle}{H} \frac{1}{x} S(Y^2 - Y_{\text{eq}}^2), \quad (3.17)$$

where $x \equiv T/m_F$ and T is the temperature of the universe. $\langle\sigma v\rangle = \langle\sigma v\rangle(x)$ is the thermal-averaged cross section discussed later. n_{eq} is the density in the thermal equilibrium, and becomes

$$n_{\text{eq}} = g_{\text{eff}} \left(\frac{m_F T}{2\pi} \right)^{3/2} e^{-m_F/T} \quad (3.18)$$

($g_{\text{eff}} = 2 \cdot 4n_F$ is the degree of freedom of the dark fermions) in the non-relativistic limit. Defining $\Delta \equiv Y - Y_{\text{eq}}$ and $\Delta' \equiv d\Delta/dx$, $Y'_{\text{eq}} \equiv dY_{\text{eq}}/dx$, we rewrite (3.17) as

$$\Delta' = -Y'_{\text{eq}} + f(x)\Delta(2Y_{\text{eq}} + \Delta), \quad f(x) = \sqrt{\frac{\pi g_*}{45}} m_F M_{Pl} \langle\sigma v\rangle, \quad (3.19)$$

which is written at early times ($x \gg x_f \equiv T_f/m_F$, $|\Delta'| \ll |Y'_{\text{eq}}|$) as

$$\Delta = \frac{Y'_{\text{eq}}}{f(x)(2Y_{\text{eq}} + \Delta)}. \quad (3.20)$$

At late times ($T \ll T_f$), $Y_{\text{eq}} \ll Y \sim \Delta$ and $|\Delta'| \gg |Y'_{\text{eq}}|$, hence (3.19) reads

$$\Delta^{-2}\Delta' = f(x). \quad (3.21)$$

Integrating (3.21) with x from zero to $x_f \equiv T_f/m_F$, we obtain

$$Y_0^{-1} \simeq \Delta_0^{-1} = \int_0^{x_f} f(x)dx = \sqrt{\frac{\pi g_*}{45}} M_{Pl} m_F J_f, \quad J_f \equiv \int_0^{x_f} \langle \sigma_{\text{eff}} v \rangle(x) dx, \quad (3.22)$$

where we have used $\Delta(x_f) \gg \Delta(x=0)$. Thus the relic density of the dark fermions at the present time is given by

$$\Omega_{DM} h^2 = \frac{\rho_{DM}}{\rho_c} h^2 = \frac{m_F S_0 Y_0 h^2}{\rho_c} = \frac{1.04 \times 10^9}{M_{Pl}} \frac{1}{\sqrt{g_*}} \frac{1}{J_f}, \quad (3.23)$$

where $\rho_{DM} = m_F S_0 Y_0$ and $\rho_c = 3H_0^2 M_{Pl}^2 / 8\pi = 1.054 \times 10^{-5} \text{GeVcm}^{-3}$ have been made use of. $S_0 = 2889.2 \text{cm}^{-3}$ is the entropy-density of the present universe.

The freeze-out temperature is determined by solving the condition

$$\Delta(x_f) = c Y_{\text{eq}}(x_f), \quad (3.24)$$

with Δ in the early-time. c is a numerical factor of order unity and determined by matching the late-time and early-time solutions. Hereafter we take $c = 1/2$. Eq. (3.24) with (3.20) reads the following transcendental relation

$$x_f^{-1} = \ln \left(c(c+2) \sqrt{\frac{45}{8}} \frac{g_{\text{eff}}}{2\pi^3} \frac{m_F M_{Pl} x_f^{1/2} \langle \sigma_{\text{eff}} v \rangle}{g_*^{1/2}} \right), \quad (3.25)$$

which can be solved by numerical iteration.

The precise form of the velocity-averaged cross section $\langle \sigma v \rangle$ is given in Ref. [74]. When σv is expanded in v^2 as

$$\sigma v = a + bv^2 + \dots = a + b[(s - 4m_F^2)/m_F^2] + \dots, \quad (3.26)$$

we obtain

$$\begin{aligned} \langle \sigma v \rangle &= 4\pi \left(\frac{m_F}{4\pi T} \right)^{3/2} \int_0^\infty dv v^2 e^{-m_F v^2 / 4T} \sigma v \\ &= a + 6bT/m_F + \dots \end{aligned} \quad (3.27)$$

In the present case $x_f \sim 1/30$ and therefore only the first term in the v^2 expansion in Eq. (3.26) is kept in the following analysis.

Table 2: θ_H , c_{top} , c_F and m_F for z_L and $n_F = 3, 4, 5$ and 6, in the case where dark fermions are degenerate.

n_F	z_L	θ_H	c_{top}	c_F	m_F [TeV]
3	10^8	0.360	0.357	0.385	0.670
	10^6	0.177	0.296	0.309	1.54
	10^5	0.117	0.227	0.235	2.54
	2×10^4	0.0859	0.137	0.127	3.88
4	10^8	0.355	0.357	0.423	0.567
	10^6	0.174	0.292	0.374	1.27
	10^5	0.115	0.227	0.332	2.03
	3×10^4	0.0917	0.168	0.299	2.66
	10^4	0.0737	0.0366	0.256	3.46
6	10^8	0.348	0.356	0.461	0.455
	10^6	0.171	0.292	0.434	1.00
	10^5	0.113	0.227	0.414	1.57
	10^4	0.0724	0.0365	0.379	2.57

3.3 Relic density of degenerate dark fermions

First we consider the case in which all dark fermions are degenerate. In the numerical study of this paper, we have adopted $\alpha_{EM} \equiv e^2/4\pi = 1/128$, $\sin^2 \theta_W = 0.2312$, $m_Z = 91.1876$ GeV and $m_{\text{top}} = 171.17$ GeV.[75] In Table. 2, we have summarized values of θ_H , the bulk mass parameters of the top quark c_{top} and the dark fermion c_F , and mass of the dark fermion m_F for particular values of (z_L, n_F) . θ_H , c_{top} and c_F are chosen so that we obtain 126GeV Higgs mass [15, 16].

In Fig. 5 the relic density of the dark fermions for $n_F = 3, 4, 5$ and 6 is plotted. In the plot, the best value [68% confidence level (CL) limits] of the relic density of the cold dark matter observed by Planck [76]:

$$\Omega_{\text{CDM}} h^2 = 0.11805 \quad [0.1186 \pm 0.0031], \quad (3.28)$$

has been also shown. Here Hubble's expansion-rate $H_0 \equiv 100h \text{ km s}^{-1} \text{ Mpc}^{-1}$, $100h = 67.11$ [67.4 ± 1.4]. In our previous work [16], we have constrained z_L by $z_L \lesssim 10^6$ because no evidence of the neutral boson resonances in LHC have been seen. For $z_L \lesssim 10^6$, we found that no parameter regions can explain the current DM density. For $n_F = 3$ we obtain $\Omega_{\text{DM}} h^2 \lesssim 0.08$ for any value of z_L . For $n_F = 4$ and $z_L \leq 10^6$, we have $\Omega_{\text{DM}} h^2 \gtrsim 0.2$. For $n_F = 5$ and 6, predicted densities are larger than the limit on the closure universe.

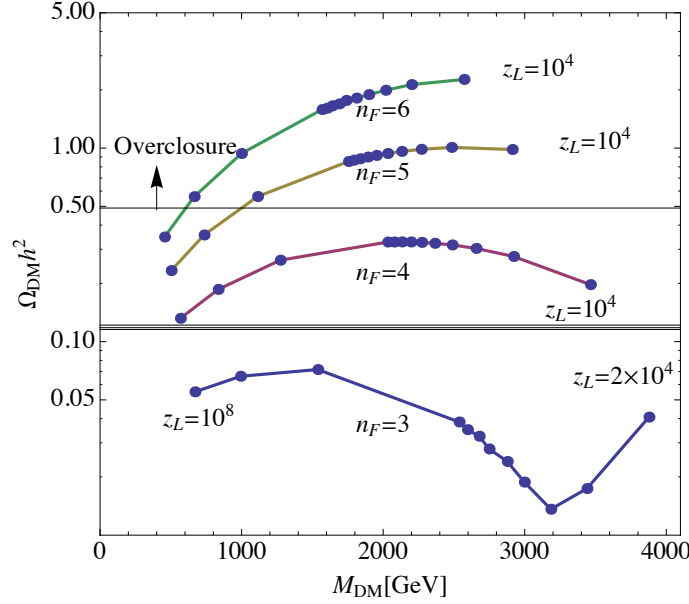


Figure 5: Relic density of neutral dark fermions in the case of n_f degenerate dark fermion multiplets ($n_F = 3, 4, 5, 6$). Data points are, from right to left, $z_L = 10^4$ (2×10^4) to 10^5 with a step of 10^4 , 10^6 , 10^7 and 10^8 for $n_F = 4, 5, 6$ ($n_F = 3$). The current observed limit of $\Omega_{\text{DM}} h^2$ and the lower bound of the over-closure of the universe are indicated as horizontal lines.

We remark that for $n_F = 3$ the relic density becomes very small at $z_L \sim 3 \times 10^4$ due to the fact that the masses of the 1st KK vector bosons are very close to twice the mass of dark fermions, and the enhancement due to the Breit-Wigner resonance happens. A similar mechanism occurs in some of the universal extra-dimension models[38, 39, 41, 42].

3.4 Current mixing

So far it has been supposed that n_F multiplets of $SO(5)$ -spinor fermions Ψ_{F_i} are degenerate. There is an intriguing scenario that some of them are heavier than others, only the lightest $F_i^{0(1)}$'s becoming the dark matter. A typical mass of $F_i^{0(1)}$ is $1 \sim 3$ TeV. We show that the mass difference of $O(200)$ GeV and small mixing could fulfill this job.

Let us denote the lightest particles of heavy and light $SO(5)$ -spinor fermions by (F_h^+, F_h^0) and (F_l^+, F_l^0) , respectively. Charged F_l^+ and F_h^+ are heavier than the corresponding neutral ones, and are supposed to decay sufficiently fast. F_h^0 also needs to decay sufficiently fast in order for the scenario to work. F_h^0 can decay either as $\rightarrow F_l^0 + Z$ or as $\rightarrow F_l^+ + W^- \rightarrow F_l^0 + W^+ + W^-$ as shown in Fig. 6. For this process the off-diagonal neutral or charged current is necessary. We examine in this subsection how the off-diagonal currents are generated.

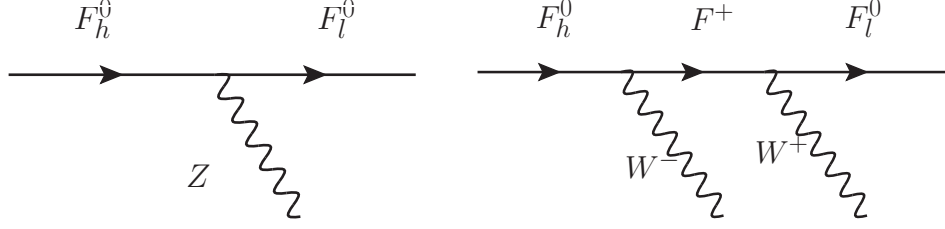


Figure 6: F_h^0 decay to F_l^0 by emitting one Z boson or two W bosons.

To be concrete, let us suppose that there are only two $SO(5)$ -spinor fermion multiplets, Ψ_{F_h} and Ψ_{F_l} , which are gauge-eigenstates. We suppose that Ψ_{F_l} obeys the boundary condition $\eta_{F_l} = +1$ in (2.5), whereas Ψ_{F_h} satisfies the flipped boundary condition $\eta_{F_h} = -1$. It is easy to confirm that their KK spectrum is given by (B.7) for both Ψ_{F_h} and Ψ_{F_l} . The lowest mode $(F_h^{+(1)}, F_h^{0(1)})$ is mostly an $SU(2)_L$ doublet, whereas $(F_l^{+(1)}, F_l^{0(1)})$ is mostly an $SU(2)_R$ doublet.

Let us denote gauge (mass) eigenstates of the lightest modes of Ψ_{F_h}, Ψ_{F_l} by $\hat{F}_h^+, \hat{F}_h^0, \hat{F}_l^+, \hat{F}_l^0$ ($F_h^+, F_h^0, F_l^+, F_l^0$). The most general form of bulk mass terms for Ψ_{F_h} and Ψ_{F_l} is

$$\mathcal{L}_F^{5D \text{ mass}} = -\sigma'(y) \{ c_{F_h} \bar{\Psi}_{F_h} \Psi_{F_h} + c_{F_l} \bar{\Psi}_{F_l} \Psi_{F_l} \} - \tilde{\Delta} \{ \bar{\Psi}_{F_h} \Psi_{F_l} + \bar{\Psi}_{F_l} \Psi_{F_h} \}. \quad (3.29)$$

We note that $\bar{\Psi}_{F_h} \Psi_{F_h}$ and $\bar{\Psi}_{F_l} \Psi_{F_l}$ are odd under parity $y \rightarrow -y$, whereas $\bar{\Psi}_{F_h} \Psi_{F_l}$ is even. The $\tilde{\Delta}$ term induces mass mixing among \hat{F}_h^+ and \hat{F}_l^+ , and among \hat{F}_h^0 and \hat{F}_l^0 . c_{F_h} and c_{F_l} generate masses \hat{m}_h and \hat{m}_l for $(\hat{F}_h^+, \hat{F}_h^0)$ and $(\hat{F}_l^+, \hat{F}_l^0)$. We suppose that $c_{F_h} < c_{F_l}$ so that $\hat{m}_h > \hat{m}_l$. As described in Sec. 3.1, charged states acquire radiative corrections (3.5), $a \hat{m}_h$ ($a \hat{m}_l$) for \hat{F}_h^+ (\hat{F}_l^+) where a is $O(10^{-3} \sim 10^{-2})$.

Hence the mass matrices are given by

$$\begin{aligned} \mathcal{L}_F^{4D \text{ mass}} &= -(\bar{\hat{F}}_h^+, \bar{\hat{F}}_l^+) \mathcal{M}_+ \begin{pmatrix} \hat{F}_h^+ \\ \hat{F}_l^+ \end{pmatrix} - (\bar{\hat{F}}_h^0, \bar{\hat{F}}_l^0) \mathcal{M}_0 \begin{pmatrix} \hat{F}_h^0 \\ \hat{F}_l^0 \end{pmatrix}, \\ \mathcal{M}_+ &= \begin{pmatrix} (1+a)\hat{m}_h & \Delta \\ \Delta & (1+a)\hat{m}_l \end{pmatrix}, \quad \mathcal{M}_0 = \begin{pmatrix} \hat{m}_h & \Delta \\ \Delta & \hat{m}_l \end{pmatrix}. \end{aligned} \quad (3.30)$$

We suppose that $\Delta \ll \hat{m}_h, \hat{m}_l$. We diagonalize the two matrices to obtain

$$\begin{aligned} \mathcal{L}_F^{4D \text{ mass}} &= -m_{F_h^+} \bar{F}_h^+ F_h^+ - m_{F_l^+} \bar{F}_l^+ F_l^+ - m_{F_h^0} \bar{F}_h^0 F_h^0 - m_{F_l^0} \bar{F}_l^0 F_l^0, \\ \begin{pmatrix} F_h^+ \\ F_l^+ \end{pmatrix} &= V(\tfrac{1}{2}\alpha_+) \begin{pmatrix} \hat{F}_h^+ \\ \hat{F}_l^+ \end{pmatrix}, \quad \begin{pmatrix} F_h^0 \\ F_l^0 \end{pmatrix} = V(\tfrac{1}{2}\alpha_0) \begin{pmatrix} \hat{F}_h^0 \\ \hat{F}_l^0 \end{pmatrix}, \end{aligned}$$

$$\begin{pmatrix} m_{F_h^+} \\ m_{F_l^+} \end{pmatrix} = \frac{1}{2}(1+a)(\hat{m}_h + \hat{m}_l) \pm \sqrt{\frac{1}{4}(1+a)^2(\hat{m}_h - \hat{m}_l)^2 + \Delta^2} ,$$

$$V(\alpha) = \begin{pmatrix} \cos \alpha & \sin \alpha \\ -\sin \alpha & \cos \alpha \end{pmatrix} , \quad \tan \alpha_+ = \frac{2\Delta}{(1+a)(\hat{m}_h - \hat{m}_l)} . \quad (3.31)$$

The masses $(m_{F_h^0}, m_{F_l^0})$ and angle α_0 are obtained from $(m_{F_h^+}, m_{F_l^+})$ and α_+ by taking $a \rightarrow 0$.

The couplings to Z (the neutral currents) are given originally by

$$Z_\mu \sum_{F_j=F_h^+, F_l^+, F_h^0, F_l^0} \left\{ g_{F_j L}^Z \bar{F}_{jL} \gamma^\mu \hat{F}_{jL} + g_{F_j R}^Z \bar{F}_{jR} \gamma^\mu \hat{F}_{jR} \right\} . \quad (3.32)$$

Similarly the couplings to W (the charged currents) are given by

$$W_\mu \sum_{j=h,l} \left\{ g_{F_j L}^W \bar{F}_{jL}^+ \gamma^\mu \hat{F}_{jL}^0 + g_{F_j R}^W \bar{F}_{jR}^+ \gamma^\mu \hat{F}_{jR}^0 \right\} + (h.c.) . \quad (3.33)$$

We recall that (F_h^+, F_h^0) is mostly an $SU(2)_L$ doublet, whereas (F_l^+, F_l^0) is mostly an $SU(2)_R$ doublet with the boundary conditions imposed on Ψ_{F_h} and Ψ_{F_l} . Therefore $g_{F_h^0 L}^Z \gg g_{F_l^0 L}^Z$ and $g_{F_h L}^W \gg g_{F_l L}^W$ etc.. In terms of mass eigenstates the neutral current becomes

$$\begin{aligned} & (\bar{F}_{hL}^0, \bar{F}_{lL}^0) \left\{ \frac{g_{F_h^0 L}^Z + g_{F_l^0 L}^Z}{2} + \frac{g_{F_h^0 L}^Z - g_{F_l^0 L}^Z}{2} U(\alpha_0) \right\} \gamma^\mu \begin{pmatrix} F_{hL}^0 \\ F_{lL}^0 \end{pmatrix} \\ & + (\bar{F}_{hL}^+, \bar{F}_{lL}^+) \left\{ \frac{g_{F_h^+ L}^Z + g_{F_l^+ L}^Z}{2} + \frac{g_{F_h^+ L}^Z - g_{F_l^+ L}^Z}{2} U(\alpha_+) \right\} \gamma^\mu \begin{pmatrix} F_{hL}^+ \\ F_{lL}^+ \end{pmatrix} \\ & + (L \rightarrow R) , \end{aligned} \quad (3.34)$$

where

$$U(\alpha) = \begin{pmatrix} \cos \alpha & -\sin \alpha \\ -\sin \alpha & -\cos \alpha \end{pmatrix} . \quad (3.35)$$

The charged current is

$$\begin{aligned} & (\bar{F}_{hL}^+, \bar{F}_{lL}^+) \left\{ \frac{g_{F_h L}^W + g_{F_l L}^W}{2} V\left(\frac{\alpha_+ - \alpha_0}{2}\right) + \frac{g_{F_h L}^W - g_{F_l L}^W}{2} U\left(\frac{\alpha_+ + \alpha_0}{2}\right) \right\} \gamma^\mu \begin{pmatrix} F_{hL}^0 \\ F_{lL}^0 \end{pmatrix} \\ & + (L \rightarrow R) . \end{aligned} \quad (3.36)$$

We recognize that off-diagonal neutral and charged currents are generated for dark fermions obeying the distinct boundary conditions.

Table 3: Parameters in the non-degenerate case of dark fermions, $(n_F^{\text{light}}, n_F^{\text{heavy}})$. Bulk mass parameter c_{F_l} and the masses m_{F_h} and m_{F_l} of F_h and F_l are tabulated for various $\Delta c_F \equiv c_{F_l} - c_{F_h}$ (see text) and z_L . Even small Δc_F gives rise to large mass difference.

Δc_F ($n_F^{\text{light}}, n_F^{\text{heavy}}$)	z_L	0.04			0.06		
		c_{F_l}	m_{F_h} [TeV]	m_{F_l} [TeV]	c_{F_l}	m_{F_h} [TeV]	m_{F_l} [TeV]
(1,3)	10^6	0.404	1.32	1.13	0.418	1.34	1.06
	10^5	0.362	2.09	1.86	0.377	2.12	1.77
	3×10^4	0.329	2.72	2.46	0.344	2.76	2.36
	10^4	0.286	3.54	3.24	0.240	3.58	3.14
(2,2)	10^5	0.352	2.15	1.92	0.361	2.21	1.86
	10^4	0.276	3.61	3.32	0.285	3.69	3.25
(3,1)	10^5	0.342	2.21	1.98	0.346	2.30	1.95
	10^4	0.266	3.68	3.39	0.270	3.80	3.36

For small θ_H , heavy dark fermions have much larger couplings to W and Z than light dark fermions. Let us suppose that $\Delta \ll \hat{m}_h - \hat{m}_l$ so that $\frac{1}{2}\alpha_0 \sim \Delta/(\hat{m}_h - \hat{m}_l) \ll 1$ and $\alpha_+ \sim \alpha_0/(1+a) \ll 1$. The Z coupling of $F_{lL/R}^0$ is $\sim g_{F_l^0 L/R}^Z + g_{F_h^0 L/R}^Z (\frac{1}{2}\alpha_0)^2$. We assume that $(\frac{1}{2}\alpha_0)^2 \ll \sup(|g_{F_l^0 L}^Z/g_{F_h^0 L}^Z|, |g_{F_l^0 R}^Z/g_{F_h^0 R}^Z|)$ so that the estimate of the cross section for the direct detection experiments discussed in the next section remains valid.

The couplings for $F_{hL}^0 \rightarrow F_{lL}^0 + Z$ and for $F_{hL}^0 \rightarrow F_{lL}^+ + W^-$ are approximately $-\frac{1}{2}g_{F_h^0 L}^Z \alpha_0$ and $-\frac{1}{2}g_{F_h L}^W \alpha_0$, respectively. With a moderate $\frac{1}{2}\alpha_0 \sim \frac{1}{3} \sup(|g_{F_l^0 L}^Z/g_{F_h^0 L}^Z|^{1/2}, |g_{F_l^0 R}^Z/g_{F_h^0 R}^Z|^{1/2})$, F_{hL}^0 decays sufficiently fast. Only the light dark fermion F_{lL}^0 becomes a candidate of dark matter.

3.5 Relic density of non-degenerate dark fermions

Let us examine the case with non-degenerate dark fermions. We separate the n_F dark fermions (F_i^+, F_i^0) ($i = 1, \dots, n_F$) into n_F^{light} light fermions (F_l^+, F_l^0) (with bulk mass c_{F_h}) and n_F^{heavy} heavy fermions (F_h^+, F_h^0) (with c_{F_h}). Here $\Delta c_F \equiv c_{F_l} - c_{F_h} > 0$. c_{F_l} and c_{F_h} are chosen so as to keep the values of θ_H and m_H unchanged. In Table. 3, the values of c_{F_l} , Δc_F and the corresponding fermion masses are tabulated. The changes in the couplings of n_F^{light} fermions to vector bosons from those in the degenerate case are found to be small.

At the temperature $T \gtrsim m_{F_h} - m_{F_l}$, the heavy-light conversion process depicted in Fig. 7 dominates, and both F_h and F_l obey the Boltzmann distribution. When $m_{F_h} - m_{F_l} \gtrsim T_f = \mathcal{O}(100 \text{ GeV})$, the number density of F_h becomes much smaller than that of F_l .

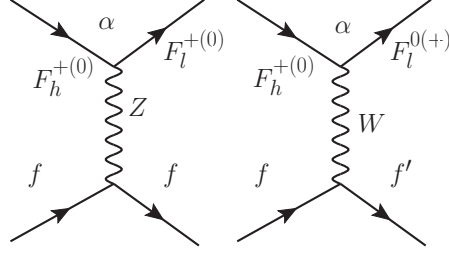


Figure 7: Dominant processes of $F_h \leftrightarrow F_l$ conversion. f and f' are the SM fermions. α denotes the suppression of the FFW , FFZ vertex factor by the mixing.

In contrast to F_l , F_h obey the boundary condition $\eta_{F_h} = -1$ and its couplings to W and Z are not suppressed, whereas its coupling to Z_R is suppressed. Thus the dominant annihilation processes of F_h are s-channel processes of $F\bar{F}$ annihilation to the SM fermions through $Z^{(1)}$ and $\gamma^{(1)}$ [(a-ii) with $V = Z^{(1)}$ and (ac-iv) with $V = \gamma^{(1)}$ in Table. 1] and co-annihilation through $W^{(1)}$ [(co-i) with $V = W^{(1)}$ in Table. 1]. The time evolutions of the total dark fermion density is given by

$$\begin{aligned}
\frac{dn}{dt} &= -3Hn - 2n_F^{\text{light}} \langle \sigma_{l0} v \rangle (n_{l0}^2 - n_{l0,\text{eq}}^2) - 2n_F^{\text{light}} \langle \sigma_{l+} v \rangle (n_{l+}^2 - n_{l+,\text{eq}}^2) \\
&\quad - 2n_F^{\text{heavy}} \langle \sigma_{h0} v \rangle (n_{h0}^2 - n_{h0,\text{eq}}^2) - 2n_F^{\text{heavy}} \langle \sigma_{h+} v \rangle (n_{h+}^2 - n_{h+,\text{eq}}^2) \\
&\quad - 4n_F^{\text{heavy}} \langle \sigma_{hc} v \rangle (n_{h0} n_{h+} - n_{h0}^{\text{eq}} n_{h+}^{\text{eq}}) \\
&= -3Hn - 2n_F^{\text{light}} \left(\frac{n_l^{\text{eq}}}{n_{\text{eq}}} \right)^2 [\langle \sigma_{l0} v \rangle + \langle \sigma_{l+} v \rangle] (n^2 - n_{\text{eq}}^2) \\
&\quad - 2n_F^{\text{heavy}} \left(\frac{n_h^{\text{eq}}}{n_{\text{eq}}} \right)^2 [\langle \sigma_{h0} v \rangle + \langle \sigma_{h+} v \rangle + 2\langle \sigma_{hc} v \rangle] (n^2 - n_{\text{eq}}^2) \\
&\equiv -3Hn - \langle \sigma_{\text{eff}}^{\text{ND}} v \rangle (n^2 - n_{\text{eq}}^2), \tag{3.37}
\end{aligned}$$

where n_{w0} and n_{w+} ($w = h, l$) are the number densities of $F_{w,i}^0$, $F_{w,i}^+$ ($i = 1, \dots, n_F^{\text{light}}$ for $w = l$, and $1, \dots, n_F^{\text{heavy}}$ for $w = h$), respectively. σ_{w0} , σ_{w+} and σ_{hc} are the cross section of $F_{w,i}^0 \bar{F}_{w,i}^0$, $F_{w,i}^+ F_{w,i}^-$ annihilations and $F_h^+ F_h^0$ co-annihilation, respectively. We also have used

$$\frac{n_{w0/+}}{n} \simeq \frac{n_{w0/+,\text{eq}}}{n_{\text{eq}}}, \quad n_{w0}^{(\text{eq})} \simeq n_{w+}^{(\text{eq})} \equiv n_w^{(\text{eq})}, \quad w = h, l. \tag{3.38}$$

The number densities in the thermal equilibrium are given by

$$\begin{aligned}
\frac{n_l^{\text{eq}}}{n_{\text{eq}}} &= \frac{1}{4n_F^{\text{light}} + 4n_F^{\text{heavy}} (1 + \eta)^{3/2} \exp(-\eta/x)}, \\
\frac{n_h^{\text{eq}}}{n_{\text{eq}}} &= \frac{(1 + \eta)^{3/2} \exp(-\eta/x)}{4n_F^{\text{light}} + 4n_F^{\text{heavy}} (1 + \eta)^{3/2} \exp(-\eta/x)}, \quad \eta \equiv \frac{m_{F_h} - m_{F_l}}{m_{F_l}}, \tag{3.39}
\end{aligned}$$

and g_{eff} in (3.18) will be replaced with

$$g_{\text{eff}}^{\text{ND}} = 2 \cdot 4n_F^{\text{light}} + 2 \cdot 4n_F^{\text{heavy}}(1 + \eta)^{3/2} \exp(-\eta/x). \quad (3.40)$$

When $\eta/x \gg 1$, the Boltzmann equation (3.37) with (3.39) can be approximated by

$$\begin{aligned} \frac{dn}{dt} &= -3Hn \langle \sigma_{\text{eff}}^{\text{ND}} v |_{\eta \rightarrow \infty} \rangle (n^2 - n_{\text{eq}}^2), \\ \sigma_{\text{eff}}^{\text{ND}} v |_{\eta \rightarrow \infty} &= \frac{1}{8n_F^{\text{light}}} [\sigma_{l0} v + \sigma_{l+v} v], \end{aligned} \quad (3.41)$$

and $g_{\text{eff}}^{\text{ND}}|_{\eta \rightarrow \infty} = 2 \cdot 4n_F^{\text{light}}$. With this approximation, one can calculate the relic density of the dark fermion by following the procedure described in Sec. 3.2. Since the effective cross section, and therefore J_f in (3.22), is enhanced by a factor $\sigma_{\text{eff}}^{\text{ND}} v |_{\eta \rightarrow \infty} / \sigma_{\text{eff}} v \simeq n_F / n_F^{\text{light}}$, which results in the reduction of the relic density by a factor n_F^{light} / n_F as seen from (3.23). If η is not so large, the approximation (3.41) is not valid any more. In particular, for $\eta \sim 0$ the Boltzmann equation (3.37) become almost identical to (3.16), and the relic density will be increased up to that in the degenerate case. Effects of small η on $\Omega_{\text{DM}} h^2$ (3.23) mainly appear in the change of the value of J_f (or $\langle \sigma_{\text{eff}} v \rangle$). Numerically we find that J_f determined from (3.41) well approximates J_f determined from (3.37) with (3.39) at $\mathcal{O}(5\%)$ accuracy when $\eta \gtrsim 0.10$ for $x = x_f \simeq 1/30$ and $\sigma_{l0/+} \sim \sigma_{h0/+}$.

We note that in the cross section (3.13), the total decay width of $Z_R^{(1)}$ (3.14) can be modified so that it consists $n_F^{\text{light}} F_l$ and $n_F^{\text{heavy}} F_h$ partial decay widths, as $Z_R F_l \bar{F}_l$ and $Z_R F_h \bar{F}_h$ couplings are not the same. The total decay width of $\gamma^{(1)}$ does not change so much, since $\gamma^{(1)} F \bar{F}$ copings are invariant under the exchange $SU(2)_L \leftrightarrow SU(2)_R$. Numerically we find the change of the cross section (3.13) induced from the change in decay widths amounts only to a few percents.

From Table. 3, we see that for $\Delta_{c_F} \gtrsim 0.04$ the condition $\eta \gtrsim 0.1$ is satisfied and the cross section formula (3.41) is valid. In Fig. 8 we have plotted the relic density of the dark fermion determined from the Boltzmann equation (3.41) for $\Delta_{c_F} = 0.04$ and 0.06 in the case of $n_F = 4$ with $(n_F^{\text{light}}, n_F^{\text{heavy}}) = (1, 3)$. For $\Delta_{c_F} < 0.04$, the approximated formula (3.41) is no more valid, and the relic-density can be much larger than those for $\Delta_{c_F} \gtrsim 0.04$. By inter-/extra-polating the $\Omega_{\text{DM}} h^2$ with respect to Δ_{c_F} and z_L , we plot the parameter region (Δ_{c_F}, z_L) allowed by the experimental limit on the current relic density in Fig. 9. It is seen that the observed current relic density is obtained when $10^4 \lesssim z_L \lesssim 10^6$ ($0.07 \lesssim \theta_H \lesssim 0.17$) in the range $0.04 \lesssim \Delta_{c_F} \lesssim 0.07$. The mass of the dark fermion m_{DM} varies within the

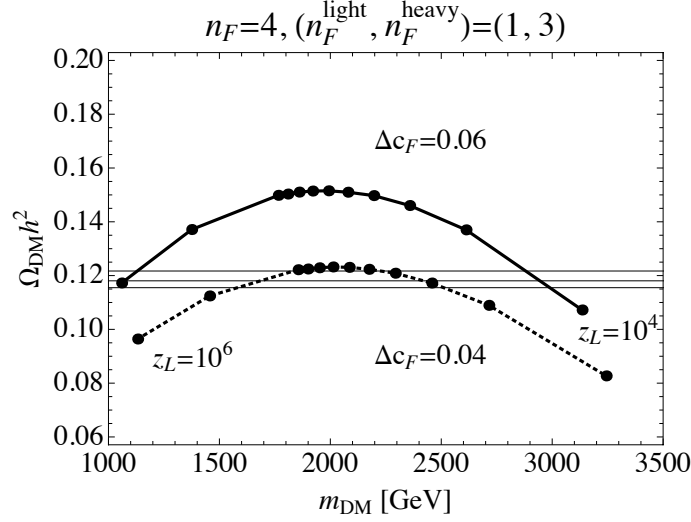


Figure 8: Relic density of the dark fermion versus $m_{\text{DM}} = m_{F_l}$ for $n_F = 4$ ($n_F^{\text{light}} = 1, n_F^{\text{heavy}} = 3$). Thick-solid and thick-dotted lines are $\Delta c_F \equiv c_{F_l} - c_{F_h} = 0.06$ and 0.04 , respectively. Data points are, from right to left, $z_L = 10^4$ to 10^5 with an interval 10^4 , 3×10^5 and 10^6 . Horizontal lines around $\Omega_{\text{DM}} h^2 \sim 0.12$ show the observed 68% confidence level (CL) limit of the relic density of the cold dark matter.

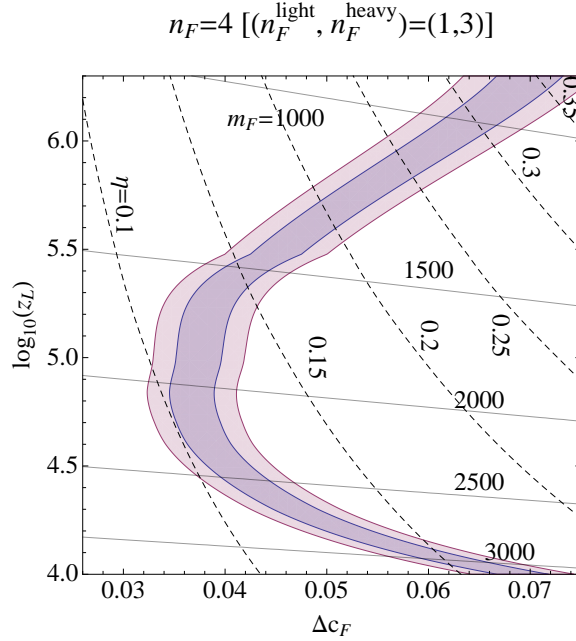


Figure 9: Parameter region $(\Delta c_F, z_L)$ allowed by the limits of relic density. Inner and outer colored regions are allowed with the 68% CL limit and twice of the 68% CL limit $\Omega_{\text{DM}} h^2 \subset [0.1186 \pm 2 \times 0.0031]$, respectively. Mass of the dark fermion m_{F_l} and a mass ratio $\eta \equiv (m_{F_h} - m_{F_l})/m_{F_l}$ are also indicated as solid and dashed lines, respectively.

range of [1000, 3100] GeV. For $n_F = 5, 6$ and $n_F = 4$ with $(n_F^{\text{light}}, n_F^{\text{heavy}}) = (2, 2), (3, 1)$, we find no parameter region which explains the current DM density.

In the numerical study we have used an approximation explained in Sec. 3.2. In the case where the Breit-Wigner resonance enhance the DM relic density, a more rigorous treatment may be required.[71] In the case under consideration, the effect of the enhancement is found to be mild. Quantitatively, in the notation of Ref. [71] we obtain $\epsilon = (\Gamma_V/m_V)^2 = \mathcal{O}(0.005)$ ($V = Z^{(1)}, Z_R^{(1)}, \gamma^{(1)}$) and $\sqrt{u} = 2m_F/m_V \lesssim 0.8$. In this parameter region the approximation can be justified.[71]

Before closing this section, we make a few comments. First we comment on the effect of dark fermions on the electroweak precision parameters [77], in particular on the S -parameter. Since the dark fermions have vector-like couplings to the Z boson, the contribution to the S parameter from an $SU(2)$ doublet $\{F^+, F^0\}$ is estimated to be

$$\Delta(\alpha_{\text{EM}}S) \simeq 4s_w^2 c_w^2 \Pi'(0) \sum_{F=F^+, F^0} \left((g_{FV}^Z)^2 - \frac{c_w^2 - s_w^2}{c_w s_w} g_{FV}^Z Q_F e - Q_F^2 e^2 \right),$$

$$c_w \equiv \cos \theta_W, \quad s_w \equiv \sin \theta_W, \quad (3.42)$$

where $g_{FV}^Z \equiv (g_{FL}^Z + g_{FR}^Z)/2$ and Q_F is the vector coupling to Z and the electric charge of F , respectively. $\Pi(p^2)$ is the vacuum polarization function which is induced by the one-loop fermion with vector-type coupling. Numerically we find that in both cases of F_l ($\eta_{F_l} = +1$) and F_h ($\eta_{F_h} = -1$) the sum of the right-hand side in (3.42) vanishes accurately. Hence there are no sizable corrections of the S parameter from dark fermions.

Secondly as an stabilization mechanism of the branes one can introduce some dynamical model a la Goldberger-Wise[78]. In such a case the phase transition of the radion field may alter the thermal history of the universe drastically[79]. Here we have supposed that the critical temperature of the radion phase transition, T_ϕ , is much higher than the freeze-out temperature of the dark fermions, e.g., $T_\phi \gg T_f \sim 100$ GeV.

4 Direct detection

In this section, we analyse the elastic scattering of the dark fermion (F^0) off a nucleus [35, 36, 80] and examine the constraint coming from direct detection experiments.[63, 64] The dominant process of the F^0 -nucleus scattering turns out the Z boson exchange, though the Z - F^0 coupling is very small. The $Z_R^{(n)}$ - F^0 coupling is larger, but $Z_R^{(n)}$ is heavy.

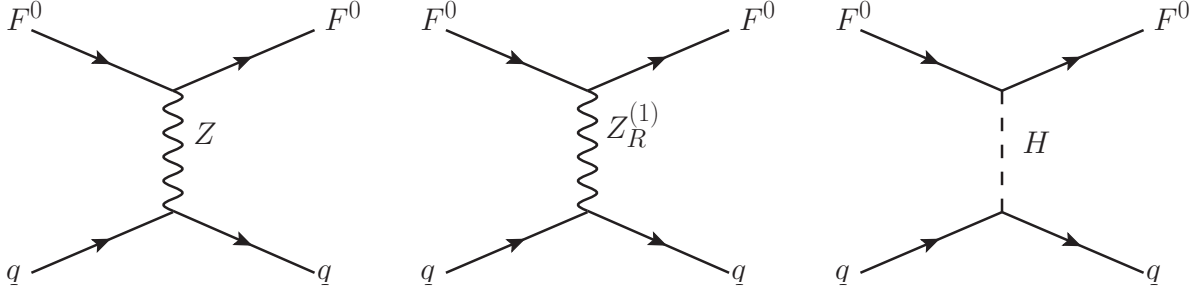


Figure 10: Dominant and subdominant processes of the F^0 -nucleus scattering

Subdominant are the processes of $Z_R^{(1)}$ and Higgs exchange. Contributions from other processes are negligible.

In the scattering of F^0 on nuclei with large mass number A , scalar and vector interactions dominate for the spin-independent cross section. Therefore the effective Lagrangian at low energies is given by

$$\mathcal{L}_{\text{int}} \simeq \sum_q \left\{ - \left(\frac{g_w^2 v_q}{m_Z^2 \cos^2 \theta_W^2} V_F + \frac{g_w^2 v_q^{(Z_R^{(1)})}}{m_{Z_R^{(1)}}^2} V_F^{(Z_R^{(1)})} \right) \bar{q} \gamma^0 q \bar{F}^0 \gamma_0 F^0 + \frac{y_q Y_F}{m_H^2} \bar{q} q \bar{F}^0 F^0 \right\}. \quad (4.1)$$

To evaluate the scattering amplitude by the Higgs exchange, we need estimate the nucleon matrix element

$$\langle N | m_q \bar{q} q | N \rangle = m_N f_{Tq}^{(N)}, \quad (4.2)$$

where $N = p, n$. For heavy quarks ($Q = c, b, t$) one has

$$f_{TQ}^{(N)} = \frac{2}{27} \left(1 - \sum_{q=u,d,s} f_{Tq}^{(N)} \right). \quad (4.3)$$

In the GHU model, quark couplings satisfy $v_q|_{\text{GHU}} \simeq v_q|_{\text{SM}}$ and

$$y_q|_{\text{GHU}} \simeq y_q|_{\text{SM}} \cos \theta_H = \frac{g_w}{2m_W} m_q \cos \theta_H, \quad (4.4)$$

to good accuracy.[21] Therefore, by dropping the small momentum dependence of the form factor, the spin-independent cross section of the F^0 -nucleus elastic scattering becomes

$$\begin{aligned} \sigma_0 &\equiv \int_0^{4M_r^2 v^2} \frac{d\sigma}{d|\mathbf{q}|^2} \Big|_{|\mathbf{q}|=0} d|\mathbf{q}|^2 \\ &= \frac{M_r^2}{\pi} \left\{ Z (b_p + f_p) + (A - Z) (b_n + f_n) \right\}^2, \end{aligned} \quad (4.5)$$

where M_r is the F^0 -nucleus reduced mass and Z (A) is the atomic (mass) number of the nucleus. $|\mathbf{q}|$ is the momentum transfer and

$$b_p = 2b_u + b_d, \quad b_n = b_u + 2b_d,$$

Table 4: F^0 mass m_F and the spin-independent cross section σ_N of the F^0 -nucleon scattering for $n_F = 4, 5, 6$ degenerate dark fermions.

$n_F = 4$			
z_L	θ_H	m_F (TeV)	σ_N (cm ²)
10^5	0.115	2.03	5.33×10^{-44}
5×10^4	0.101	2.36	3.78×10^{-44}
3×10^4	0.092	2.66	2.99×10^{-44}
2×10^4	0.085	2.92	2.53×10^{-44}
10^4	0.074	3.46	2.03×10^{-44}

$n_F = 5$			
z_L	θ_H	m_F (TeV)	σ_N (cm ²)
10^5	0.114	1.75	3.67×10^{-44}
10^4	0.073	2.91	1.01×10^{-44}

$n_F = 6$			
z_L	θ_H	m_F (TeV)	σ_N (cm ²)
10^5	0.113	1.57	2.96×10^{-44}
10^4	0.072	2.56	0.72×10^{-44}

$$b_q = -4\sqrt{2}G_F \left(v_q V_F + \frac{m_W^2}{m_{Z_R^{(1)}}^2} v_q^{(Z_R^{(1)})} V_F^{(Z_R^{(1)})} \right) ,$$

$$f_N = \frac{Y_F}{m_H^2} \sum_q \langle N | y_q \bar{q} q | N \rangle = \frac{Y_F}{m_H^2} \frac{g_w m_N}{2m_W} \cos \theta_H \left(\frac{2}{9} + \frac{7}{9} \sum_{q=u,d,s} f_{T_q}^{(N)} \right) . \quad (4.6)$$

The spin-independent cross section of the F^0 -nucleon elastic scattering σ_N can be written as

$$\sigma_N \equiv \frac{1}{A^2} \frac{m_r^2}{M_r^2} \sigma_0 , \quad (4.7)$$

where m_r is the F^0 -nucleon reduced mass.

The F^0 -nucleon cross sections σ_N are shown in Table 4 and Figure 11. In the numerical evaluation we have employed the values given by [36]

$$\begin{aligned} f_{Tu}^{(p)} &= 0.020 , \quad f_{Td}^{(p)} = 0.026 , \quad f_{Ts}^{(p)} = 0.118 , \\ f_{Tu}^{(n)} &= 0.014 , \quad f_{Td}^{(n)} = 0.036 , \quad f_{Ts}^{(n)} = 0.118 . \end{aligned} \quad (4.8)$$

Recent lattice simulations show smaller values for $f_{Ts}^{(N)}$ [81], which yields slightly smaller cross sections than those described below.

In the previous section we have seen that when all n_F dark fermions are degenerate, there are no parameter regions which reproduce the observed value of the relic DM density.

Table 5: m_{F_l} , $m_{Z_R^{(1)}}$, the couplings of F_l^0 and the spin-independent cross section σ_N of the F_l^0 -nucleon scattering for $n_F = 4$ and $(n_F^{\text{light}}, n_F^{\text{heavy}}) = (1, 3)$. V_F , $v_q^{(Z_R^{(1)})}$ ($q = u, d$), Y_F are defined in Eq. (4.1).

$\Delta c_F = 0.04$									
z_L	θ_H	m_{F_l} (TeV)	$m_{Z_R^{(1)}}$ (TeV)	V_F	$v_u^{(Z_R^{(1)})}$	$v_d^{(Z_R^{(1)})}$	$V_F^{(Z_R^{(1)})}$	Y_F	σ_N (cm ²)
4×10^4	0.097	2.29	6.47	-0.00108	0.474	-0.237	1.11	-0.0299	2.69×10^{-44}
3×10^4	0.092	2.46	6.74	-0.00100	0.469	-0.234	1.11	-0.0293	2.35×10^{-44}
2×10^4	0.085	2.72	7.15	-0.00092	0.461	-0.231	1.10	-0.0286	1.96×10^{-44}
10^4	0.074	3.24	7.92	-0.00081	0.450	-0.225	1.08	-0.0280	1.53×10^{-44}

$\Delta c_F = 0.06$									
z_L	θ_H	m_{F_l} (TeV)	$m_{Z_R^{(1)}}$ (TeV)	V_F	$v_u^{(Z_R^{(1)})}$	$v_d^{(Z_R^{(1)})}$	$V_F^{(Z_R^{(1)})}$	Y_F	σ_N (cm ²)
2×10^4	0.085	2.61	7.15	-0.00086	0.461	-0.231	1.09	-0.0266	1.76×10^{-44}
10^4	0.074	3.13	7.92	-0.00075	0.450	-0.225	1.07	-0.0261	1.35×10^{-44}

It was shown that the observed DM density can be obtained when there are n_F^{light} light dark fermions and n_F^{heavy} heavy dark fermions of opposite η_F in the boundary conditions. In particular, for the parameter set of $(n_F^{\text{light}}, n_F^{\text{heavy}}) = (1, 3)$, the region $0.04 \lesssim \Delta c_F \lesssim 0.07$, $z_L \lesssim 10^6$ successfully explains the relic abundance as shown in Fig. 9. The allowed band region in Fig. 9 is mapped in Fig. 11 for the spin-independent cross section for the F^0 -nucleon elastic scattering. The purple and light purple bands there represent the regions allowed by the limit of the relic abundance of DM at the 68 % CL and by twice of that, respectively. It is seen that the band region from $z_L = 10^4$ to 4×10^4 is allowed by the direct detection experiments of LUX [64] and XENON100 [63]. In the allowed region the dark fermion mass ranges from 3.1 TeV to 2.3 TeV, whereas the AB phase θ_H ranges from 0.074 to 0.097. The mass of Z' bosons (the lowest Z_R boson and the first KK modes $Z^{(1)}$ and $\gamma^{(1)}$) ranges from 8 TeV to 6.5 TeV. For reference we have added, in Fig. 11, the expected limit by the 300 live-days result of the LUX experiment. The XENON 1T experiment is expected to give a limit one order of magnitude smaller than that of the LUX 300 live-days experiment in the cross-section.

We remark that the $n_F = 3$ case predicts too small relic densities as shown in Fig. 8. It implies that the dark fermions in the GHU model accounts for only a fraction of the dark matter of the universe, and the model is not excluded by the direct-detection experiments.

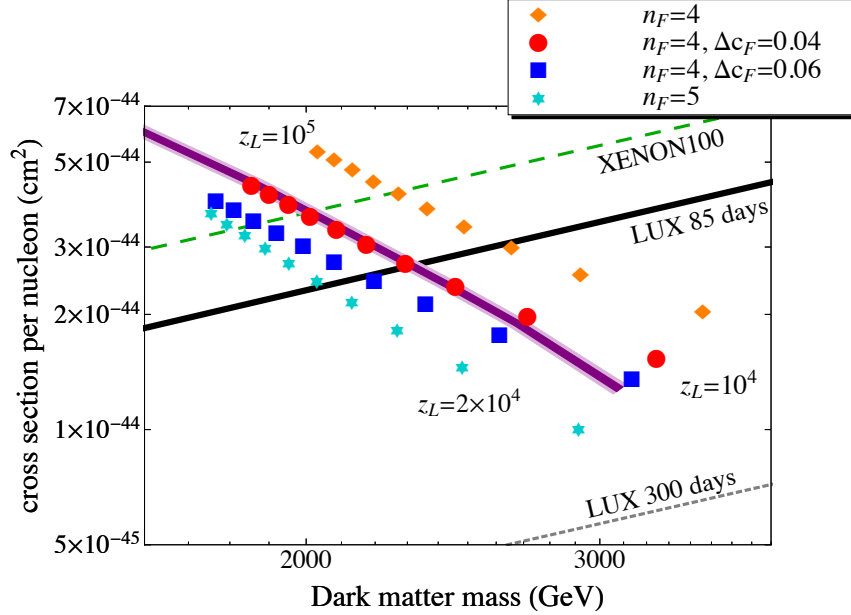


Figure 11: The spin-independent cross section of the F^0 -nucleon elastic scattering for $10^4 \leq z_L \leq 10^5$. The orange diamonds and light blue stars represent the $n_F = 4$ and $n_F = 5$ cases of degenerate dark fermions with a step of 10^4 in z_L , respectively. Red circles and blue squares represent the cases of non-degenerate dark fermions $(n_F^{\text{light}}, n_F^{\text{heavy}}) = (1, 3)$ with $\Delta c_F = 0.04$ and 0.06 , respectively. The black solid line and green dashed line are the 90% confidence limits set by the 85.3 live-days result of the LUX experiment[64] and the 225 live-days result of the XENON100 experiment[63], respectively. For reference we have added the expected limit by the 300 live-days result of the LUX experiment. The XENON 1T experiment is expected to give a limit one order of magnitude smaller than that of the LUX 300 live-days experiment in the cross-section. The purple and light purple bands represent the regions allowed by the limit of the relic density of DM at the 68 % CL depicted in Fig. 9 and by twice of that. The model with dark fermions of $2.3 \text{ TeV} < m_{F_l} < 3.1 \text{ TeV}$ ($4 \times 10^4 > z_L > 10^4$) gives a consistent scenario.

5 Conclusion and discussions

In the present paper we have given a detailed analysis of DM in GHU. In the $SO(5) \times U(1)$ GHU, the observed unstable Higg boson is realized by introducing $SO(5)$ -spinor fermions. Spinor fermions do not directly interact with $SO(5)$ -vector fermions which contain the SM quarks and leptons. Therefore the total spinor-fermion number is conserved and the lightest one can remain as dark matter in the current universe. Such fermions are referred to as “dark fermions”.

In Sec. 3 we have evaluated the relic density of the dark fermions. Although charged and neutral dark fermions are degenerate at tree level, charged fermions become heavier

than neutral ones through loop effects so that the charged dark fermions decay into neutral ones much earlier than they cooled down at their freeze-out temperature. We found that among various annihilation processes of dark fermions dominant ones are those in which a dark fermion and its antiparticle annihilate into the SM fermions mediated by the lowest KK Z_R boson and the first KK photon. We also have evaluated the annihilation cross section and obtained the relic densities of the dark fermions in the current universe for the various values of n_F and z_L . The results depend sensitively on the number of dark fermions n_F . When all neutral dark fermions are degenerate, no solution has been found which explains the observed value of the relic density of dark matter and is consistent with the limit from the direct detection experiments. For $n_F = 3$ the relic density becomes much smaller than the bound, because twice the mass of the dark fermion is close to the mass of the Z_R boson and the annihilation is enhanced by the resonance. For $n_F = 4, 5$ and 6 the relic density becomes larger than the bound.

We have considered the case in which n_F dark fermions consist of n_F^{light} lighter fermions and n_F^{heavy} heavier fermions. They are mixed with each other through the bulk mass terms which can be introduced when lighter and heavier fermions have opposite signs of η_F in the boundary conditions under reflections at the TeV and Planck branes. When the mass difference of these fermions are sufficiently large (more than $\mathcal{O}(100\text{GeV})$), heavier ones decay quickly to lighter ones and the effective number of species of the dark fermions can be reduced from n_F to n_F^{light} . Accordingly the relic density reduces to n_F^{light}/n_F of that in the degenerate case. For $n_F = 4$ it is found that one can obtain the relic density consistent with the experimental bound for $10^4 \lesssim z_L \lesssim 10^6$, $0.04 \lesssim \Delta c_F \lesssim 0.07$ when $(n_F^{\text{light}}, n_F^{\text{heavy}}) = (1, 3)$. In the cases of $(n_F^{\text{light}}, n_F^{\text{heavy}}) = (2, 2), (3, 1)$ and of $n_F = 5$ and $= 6$ no solution has been found. We comment that there are no sizable corrections to the S -parameter from the dark-fermion loops.

In Sec. 4, we calculated the scattering cross section of the dark fermions with nucleons. The dark fermions have very small Higgs-Yukawa couplings and Z -boson couplings, both of which are suppressed by powers of $\sin \theta_H$. We evaluated the spin-independent cross sections and compared with the experimental bound obtained in the recent experiments of WIMP direct detection.[63, 64] Combining with the constraint from the relic density, we showed that the region $10^4 \lesssim z_L \lesssim 4 \times 10^4$ for $(n_F^{\text{light}}, n_F^{\text{heavy}}) = (1, 3)$ is viable. The corresponding mass of the dark matter candidate (dark fermions) ranges from 3.1 TeV to 2.3 TeV, whereas the AB phase θ_H ranges from 0.074 to 0.097. The mass of Z' bosons ranges from 8 TeV to 6.5 TeV.

The $n_F = 4$ model with one light and three heavy dark fermions with opposite boundary conditions is consistent with the current direct detection experiments. Such dark fermions should be detected in the direct-detection experiments in near future. For $n_F = 3$, our model cannot explain the current DM density. In this case the current DM density should be accounted for by dark matter generated by other mechanism such as axion DM [51] and dynamical dark matter [58]. In this case DM in the GHU model may or may not be detected, depending on the property of the dominant dark matter components.

The gauge-Higgs unification scenario is viable and promising. The $SO(5) \times U(1)$ GHU predicts new Z' bosons in the 6.5 TeV \sim 8 TeV region and deviation of the self-couplings of the Higgs boson from SM, which can be explored and checked at the upgraded LHC and ILC experiments. We stress again that the model naturally contains the dark matter candidate (dark fermions) in the mass range 2.3 TeV \sim 3.1 TeV. The mass and cross section of the dark fermions are within the reach of the ongoing and future experiments, and the allowed parameter region of this model can be explored with future collider experiments [16]. Pinning down its mass fixes the value of θ_H , which further yields more predictions of GHU in collider experiments.

Acknowledgements

We thank Mitsuru Kakizaki and Minoru Tanaka for many valuable comments. This work was supported in part by JSPS KAKENHI grants, No. 23104009 (YH and YO), No. 21244036 (YH) and No. 2518610 (TS), and NRF Research Grant 2012R1A2A1A01006053 (HH), No. 2009-0083526 (YO) of the Republic of Korea.

A $SO(5)$ generators and base functions

$SO(5)$ generators in the spinorial representation are defined as

$$T_L^a = \frac{1}{2} \begin{pmatrix} \sigma^a \\ \end{pmatrix}, \quad T_R^a = \frac{1}{2} \begin{pmatrix} \end{pmatrix} \sigma^a, \quad (\text{A.1})$$

$$\hat{T}^a = \frac{1}{2\sqrt{2}} \begin{pmatrix} & i\sigma^a \\ -i\sigma^a & \end{pmatrix}, \quad \hat{T}^4 = \frac{1}{2\sqrt{2}} \begin{pmatrix} & I \\ I & \end{pmatrix}, \quad (\text{A.2})$$

and $\text{Tr}[T^\alpha, T^\beta] = \delta^{\alpha\beta}$ holds.

Mode functions for KK towers are expressed in terms of Bessel functions. For gauge fields we define

$$C(z; \lambda) = \frac{\pi}{2} \lambda z z_L F_{1,0}(\lambda z, \lambda z_L), \quad C''(z; \lambda) = \frac{\pi}{2} \lambda^2 z z_L F_{0,0}(\lambda z, \lambda z_L),$$

$$\begin{aligned}
S(z; \lambda) &= -\frac{\pi}{2} \lambda z F_{1,1}(\lambda z, \lambda z_L) , \quad S'(z; \lambda) = -\frac{\pi}{2} \lambda^2 z F_{0,1}(\lambda z, \lambda z_L) , \\
\hat{S}(z; \lambda) &= \frac{C(1; \lambda)}{S(1; \lambda)} S(z; \lambda) , \\
F_{\alpha, \beta}(u, v) &= J_\alpha(u) Y_\beta(v) - Y_\alpha(u) J_\beta(v) .
\end{aligned} \tag{A.3}$$

These functions satisfy

$$\begin{aligned}
C(z_L; \lambda) &= z_L , \quad C'(z_L; \lambda) = 0 , \quad S(z_L; \lambda) = 0 , \quad S'(z_L; \lambda) = \lambda , \\
CS' - SC' &= \lambda z .
\end{aligned} \tag{A.4}$$

For fermions with a bulk mass parameter c we define

$$\begin{aligned}
\begin{pmatrix} C_L \\ S_L \end{pmatrix} (z; \lambda, c) &= \pm \frac{\pi}{2} \lambda \sqrt{z z_L} F_{c+\frac{1}{2}, c \mp \frac{1}{2}}(\lambda z, \lambda z_L) , \\
\begin{pmatrix} C_R \\ S_R \end{pmatrix} (z; \lambda, c) &= \mp \frac{\pi}{2} \lambda \sqrt{z z_L} F_{c-\frac{1}{2}, c \pm \frac{1}{2}}(\lambda z, \lambda z_L) .
\end{aligned} \tag{A.5}$$

They satisfy

$$D_+(c) \begin{pmatrix} C_L \\ S_L \end{pmatrix} = \lambda \begin{pmatrix} S_R \\ C_R \end{pmatrix} , \quad D_-(c) \begin{pmatrix} C_R \\ S_R \end{pmatrix} = \lambda \begin{pmatrix} S_L \\ C_L \end{pmatrix} , \quad D_\pm(c) = \pm \frac{d}{dz} + \frac{c}{z} , \tag{A.6}$$

and

$$\begin{aligned}
C_R = C_L = 1 , \quad S_R = S_L = 0 , \quad \text{at } z = z_L , \\
C_L C_R - S_L S_R = 1 .
\end{aligned} \tag{A.7}$$

B Wave functions of dark fermions

The dark fermion Ψ_{F_i} is introduced in the spinorial representation of $SO(5)$. With the charge assignment of $Q_E = T^{3L} + T^{3R} + Q_X$ and $Q_X = \frac{1}{2}$, $\Psi_{F_i}(x, z)$ is decomposed into KK modes $F_i^{+(n)}(x)$ and $F_i^{0(n)}(x)$ ($n = 1, 2, 3, \dots$) in the twisted gauge in which $\langle A_z \rangle$ vanishes.

$$\begin{aligned}
\Psi_{F_i} &= \Psi_{F_i, R} + \Psi_{F_i, L} = \sum_n \Psi_{F_i}^{(n)} , \quad \Psi_{F_i}^{(n)} = \Psi_{F_i, R}^{(n)} + \Psi_{F_i, L}^{(n)} , \\
\gamma^5 \begin{pmatrix} \Psi_{F_i, R} \\ \Psi_{F_i, L} \end{pmatrix} &= \begin{pmatrix} +\Psi_{F_i, R} \\ -\Psi_{F_i, L} \end{pmatrix} , \\
\Psi_{F_i, R}^{(n)}(x, z) &= \sqrt{k} z^2 \left\{ \begin{pmatrix} f_{i, lR}^{(n)}(z) \\ 0 \\ f_{i, rR}^{(n)}(z) \\ 0 \end{pmatrix} F_{i, R}^{+(n)}(x) + \begin{pmatrix} 0 \\ f_{i, lR}^{(n)}(z) \\ 0 \\ f_{i, rR}^{(n)}(z) \end{pmatrix} F_{i, R}^{0(n)}(x) \right\} ,
\end{aligned}$$

$$\Psi_{F_i,L}^{(n)}(x,z) = \sqrt{k}z^2 \left\{ \begin{pmatrix} f_{i,LL}^{(n)}(z) \\ 0 \\ f_{i,rL}^{(n)}(z) \\ 0 \end{pmatrix} F_{i,L}^{+(n)}(x) + \begin{pmatrix} 0 \\ f_{i,LL}^{(n)}(z) \\ 0 \\ f_{i,rL}^{(n)}(z) \end{pmatrix} F_{i,L}^{0(n)}(x) \right\}. \quad (\text{B.1})$$

Here the suffixes l and r refer to two $SU(2)$'s of $SO(4) = SU(2)_L \times SU(2)_R \subset SO(5)$.

Ψ_{F_i} in the twisted gauge satisfies a free Dirac equation. The left- and right-handed components of $\tilde{\Psi}_{F_i} = z^{-2}\Psi_{F_i}$ satisfy

$$\begin{aligned} \sigma \cdot \partial \tilde{\Psi}_{F_i,L} &= kD_-(c) \tilde{\Psi}_{F_i,R}, \\ \bar{\sigma} \cdot \partial \tilde{\Psi}_{F_i,R} &= kD_+(c) \tilde{\Psi}_{F_i,L}. \end{aligned} \quad (\text{B.2})$$

Let us denote the $SU(2)_L$ ($SU(2)_R$) component of $\Psi_{F_i,L}$ by $\Psi_{F_i,LL}$ ($\Psi_{F_i,rL}$), etc. The boundary condition for Ψ_{F_i} with $\eta_{F_i} = +1$ in (2.5) is transformed in the twisted gauge in the coformal coordinates to

$$\begin{aligned} \cos \frac{1}{2}\theta_H \tilde{\Psi}_{F_i,LL}(1) - i \sin \frac{1}{2}\theta_H \tilde{\Psi}_{F_i,rL}(1) &= 0, \\ -i \sin \frac{1}{2}\theta_H \tilde{\Psi}_{F_i,lR}(1) + \cos \frac{1}{2}\theta_H \tilde{\Psi}_{F_i,rR}(1) &= 0, \\ \cos \frac{1}{2}\theta_H D_- \tilde{\Psi}_{F_i,lR}(1) - i \sin \frac{1}{2}\theta_H D_- \tilde{\Psi}_{F_i,rR}(1) &= 0, \\ -i \sin \frac{1}{2}\theta_H D_+ \tilde{\Psi}_{F_i,LL}(1) + \cos \frac{1}{2}\theta_H D_+ \tilde{\Psi}_{F_i,rL}(1) &= 0, \end{aligned} \quad (\text{B.3})$$

$$\begin{aligned} \tilde{\Psi}_{F_i,lR}(z_L) &= 0, \quad D_+ \tilde{\Psi}_{F_i,LL}(z_L) = 0, \\ D_- \tilde{\Psi}_{F_i,rR}(z_L) &= 0, \quad \tilde{\Psi}_{F_i,rL}(z_L) = 0, \end{aligned} \quad (\text{B.4})$$

By making use of (B.4), eigenmodes can be written as

$$\begin{aligned} \begin{pmatrix} \tilde{\Psi}_{F_i,LL}(z) \\ \tilde{\Psi}_{F_i,rL}(z) \end{pmatrix} &= \begin{pmatrix} A_1 C_L(z; \lambda, c_{F_i}) \\ B_1 S_L(z; \lambda, c_{F_i}) \end{pmatrix}, \\ \begin{pmatrix} \tilde{\Psi}_{F_i,lR}(z) \\ \tilde{\Psi}_{F_i,rR}(z) \end{pmatrix} &= \begin{pmatrix} A_2 S_R(z; \lambda, c_{F_i}) \\ B_2 C_R(z; \lambda, c_{F_i}) \end{pmatrix}. \end{aligned} \quad (\text{B.5})$$

Then (B.3) leads to

$$\begin{aligned} M \begin{pmatrix} A_1 \\ B_1 \end{pmatrix} &= M \begin{pmatrix} A_2 \\ B_2 \end{pmatrix} = 0, \\ M &= \begin{pmatrix} \cos \frac{1}{2}\theta_H C_L(1) & -i \sin \frac{1}{2}\theta_H S_L(1) \\ -i \sin \frac{1}{2}\theta_H S_R(1) & \cos \frac{1}{2}\theta_H C_R(1) \end{pmatrix}, \end{aligned} \quad (\text{B.6})$$

where $C_L(z) = C_L(z; \lambda, c_{F_i})$, $S_R(z) = S_R(z; \lambda, c_{F_i})$ etc.

The mass spectrum $\{m_{F_i,n} = k\lambda_{i,n}\}$ is determined by $\det M = 0$, or by

$$C_L(1; \lambda_{i,n}, c_{F_i})C_R(1; \lambda_{i,n}, c_{F_i}) - \sin^2 \frac{\theta_H}{2} = 0. \quad (\text{B.7})$$

The corresponding wave functions are given by

$$\begin{aligned} \begin{pmatrix} f_{i,LL}^{(n)}(z) \\ f_{i,LR}^{(n)}(z) \end{pmatrix} &= \frac{i \sin \frac{1}{2} \theta_H S_L(1)}{\sqrt{r_i^{(n)}}} \begin{pmatrix} C_L(z) \\ S_R(z) \end{pmatrix} = \frac{\cos \frac{1}{2} \theta_H C_R(1)}{\sqrt{r_i'^{(n)}}} \begin{pmatrix} C_L(z) \\ S_R(z) \end{pmatrix}, \\ \begin{pmatrix} f_{i,RL}^{(n)}(z) \\ f_{i,RR}^{(n)}(z) \end{pmatrix} &= \frac{\cos \frac{1}{2} \theta_H C_L(1)}{\sqrt{r_i^{(n)}}} \begin{pmatrix} S_L(z) \\ C_R(z) \end{pmatrix} = \frac{i \sin \frac{1}{2} \theta_H S_R(1)}{\sqrt{r_i'^{(n)}}} \begin{pmatrix} S_L(z) \\ C_R(z) \end{pmatrix}, \end{aligned} \quad (\text{B.8})$$

with $\lambda = \lambda_{i,n}$. The normalization factors $r_i^{(n)}$ and $r_i'^{(n)}$ are determined by the condition

$$\int_1^{z_L} dz \{ |f_{iL}^{(n)}|^2 + |f_{iR}^{(n)}|^2 \} = \int_1^{z_L} dz \{ |f_{iL}^{(n)}|^2 + |f_{iR}^{(n)}|^2 \} = 1 \quad (\text{B.9})$$

to be

$$\begin{aligned} r_i^{(n)} &= \int_1^{z_L} dz \{ \sin^2 \frac{1}{2} \theta_H S_L(1)^2 C_L(z)^2 + \cos^2 \frac{1}{2} \theta_H C_L(1)^2 S_L(z)^2 \} \\ &= \int_1^{z_L} dz \{ \sin^2 \frac{1}{2} \theta_H S_L(1)^2 S_R(z)^2 + \cos^2 \frac{1}{2} \theta_H C_L(1)^2 C_R(z)^2 \}, \\ r_i'^{(n)} &= \int_1^{z_L} dz \{ \cos^2 \frac{1}{2} \theta_H C_R(1)^2 C_L(z)^2 + \sin^2 \frac{1}{2} \theta_H S_R(1)^2 S_L(z)^2 \} \\ &= \int_1^{z_L} dz \{ \cos^2 \frac{1}{2} \theta_H C_R(1)^2 S_R(z)^2 + \sin^2 \frac{1}{2} \theta_H S_R(1)^2 C_R(z)^2 \}. \end{aligned} \quad (\text{B.10})$$

One comment is in order about the $\theta_H \rightarrow 0$ limit of the wave functions. For $\theta_H = 0$ the spectrum (B.7) is determined by either $C_R(1) = C_R(1; \lambda_{i,2n-1}, c_{F_i}) = 0$ or $C_L(1) = C_L(1; \lambda_{i,2n}, c_{F_i}) = 0$ ($n = 1, 2, 3, \dots$) where eigenvalues have been ordered as $0 < \lambda_{i,1} < \lambda_{i,2} < \lambda_{i,3} < \dots$. The case $C_R(1) = 0$ corresponds to excitations of the $SU(2)_R$ doublet component, whereas $C_L(1) = 0$ to excitations of the $SU(2)_L$ doublet component. For $C_R(1) = 0$ ($C_L(1) = 0$), $r_i^{(n)} / \sin^2 \frac{1}{2} \theta_H \neq 0$ ($r_i'^{(n)} / \sin^2 \frac{1}{2} \theta_H \neq 0$) at $\theta_H = 0$.

In the boundary condition for Ψ_{F_i} , one could adopt $\eta_{F_i} = -1$ in (2.5). In the case of non-degenerate dark fermions the heavy dark fermion multiplet satisfies this flipped boundary condition. In this case the corresponding wave functions and Kaluza-Klein masses are obtained from the above formulas by the replacement

$$c_H \leftrightarrow i s_H, \quad C_L \leftrightarrow S_L, \quad S_R \leftrightarrow C_R. \quad (\text{B.11})$$

The spectrum is determined by the same equation as in (B.7). The lowest mode mostly becomes an $SU(2)_L$ doublet for small θ_H .

C Gauge and Higgs couplings of dark fermions

C.1 Couplings to the Higgs boson

Couplings to the Higgs boson is read from the gauge interaction

$$\int_1^{z_L} dz \sqrt{G} e_4^z \bar{\Psi}_F (g_A A_z + Q_X g_B B_z) i \gamma_5 \Psi_F, \quad \sqrt{G} e_4^z g_A = \frac{\sqrt{L} g_w}{k^4 z^4}, \quad (\text{C.1})$$

where

$$\begin{aligned} A_z(x, z) &= \hat{H} + \sum_{a=1}^3 \hat{G}^a + \sum_{a=1}^3 \hat{D}^a, \\ \hat{H} &= \sum_n H^{(n)}(x) u_{H^{(n)}} T^{\hat{4}}, \\ \hat{G}^a &= \sum_n G^{a(n)}(x) \left\{ u_{G^{(n)}} \frac{T^{a_L} + T^{a_R}}{\sqrt{2}} \right\}, \\ \hat{D}^a &= \sum_n D^{a(n)}(x) \left\{ u_{D^{(n)}}^- \frac{T^{a_L} - T^{a_R}}{\sqrt{2}} + \hat{u}_{D^{(n)}} T^{\hat{a}} \right\}, \\ B_z(x, z) &= \sum_n B^{(n)}(x) u_{B^{(n)}}(z), \end{aligned} \quad (\text{C.2})$$

$G^{a(n)}$, $D^{a(n)}$ and $B^{(n)}$ are NG-bosons and only the \hat{H} is the tower of the physical scalar particles. Hereafter we consider only Higgs couplings. The Higgs wave functions are given by

$$u_{H^{(0)}}(z) = \sqrt{\frac{2}{k(z_L^2 - 1)}} z, \quad (\text{C.3})$$

for the zero-mode Higgs boson and

$$u_{H^{(n)}}(z) = \frac{1}{\sqrt{r_{H^{(n)}}}} S'(z; \lambda_{H^{(n)}}), \quad r_{H^{(n)}} = \int_1^{z_L} \frac{k dz}{z} S'(z; \lambda_{H^{(n)}})^2, \quad (\text{C.4})$$

for KK excitations ($n \geq 1$). Here $S(1; \lambda_{H^{(n)}}) = 0$ is satisfied. The building-block for the $H \bar{F}^{(n)} F^{(n)}$ Yukawa coupling is given by

$$\bar{\Psi}_{F_j}^{(n)} \gamma_5 T^{\hat{4}} \Psi_{F_j}^{(n)} = i \frac{k z^4}{2\sqrt{2} r_j^{(n)}} \sin \frac{\theta_H}{2} \cos \frac{\theta_H}{2} S_L(1) C_L(1) [\bar{F}_{jL}^{(n)} F_{jR}^{(n)} - \bar{F}_{jR}^{(n)} F_{jL}^{(n)}], \quad (\text{C.5})$$

where $C_L(z) C_R(z) - S_L(z) S_R(z) = 1$ has been made use of. Hence the Higgs Yukawa coupling in the 4D Lagrangian, $\mathcal{L}_{4D} \supset y_{F_i^{(n)}} H^{(0)} \bar{F}_i^{(n)} F_i^{(n)}$, is given by

$$y_{F_i^{(n)}} = \frac{g_w}{4} \frac{1}{r_i^{(n)}} \sqrt{kL(z_L^2 - 1)} \sin \frac{\theta_H}{2} \cos \frac{\theta_H}{2} S_L(1; \lambda_{i,n}, c_F) C_L(1; \lambda_{i,n}, c_F), \quad (\text{C.6})$$

In Tables 6 and 7, we have summarized the Higgs Yukawa couplings of F . In Table 7 the couplings in non-degenerate cases are summarized.

Table 6: The Higgs-Yukawa couplings $y_{F_i^{(1)}}$ in (C.6) in the case of degenerate dark fermions with the parameters specified in Table 2.

n_F	z_L	$y_{F_i^{(1)}}$
3	10^8	-0.106
	10^6	-0.071
	10^5	-0.064
	2×10^4	-0.089
4	10^8	-0.082
	10^6	-0.049
	10^5	-0.038
	3×10^4	-0.034
	10^4	-0.033
6	10^8	-0.060
	10^6	-0.034
	10^5	-0.024
	10^4	-0.017

Table 7: The Higgs-Yukawa couplings $y_{F_l^{(1)}}$ of the light dark fermion in (C.6) in the case of non-degenerate $(n_F^{\text{light}}, n_F^{\text{heavy}}) = (1, 3)$ dark fermions with the parameters specified in Table 3.

Δc_F	z_L	$y_{F_l^{(1)}}$
0.04	10^6	-0.042
	10^5	-0.033
	3×10^4	-0.029
	10^4	-0.028
0.06	10^6	-0.038
	10^5	-0.030
	3×10^4	-0.027
	10^4	-0.026

C.2 Couplings to vector bosons

Couplings to the vector bosons are read off from the gauge interaction in the 5D action

$$\int_0^{z_L} dz \sqrt{G} e_m^\mu \bar{\Psi}_F \gamma^m (g_A A_\mu + Q_X g_B B_\mu) \Psi_F, \quad \sqrt{G} e_m^\mu g_A = \frac{g_w \sqrt{L}}{k z^4} \delta_m^\mu, \quad (\text{C.7})$$

where $A_\mu(x, z)$ and $B_\mu(x, z)$ decompose to the Kaluza-Klein towers

$$\begin{aligned} A_\mu(x, z) &= \hat{W}_\mu^- + \hat{W}_\mu^+ + \hat{Z}_\mu^{(A)} + \hat{A}_\mu^{\gamma(A)} + \hat{W}_{R\mu}^- + \hat{W}_{R\mu}^+ + \hat{Z}_{R\mu}^{(A)} + \hat{A}_\mu^{\hat{4}}, \\ B_\mu(x, z) &= \hat{Z}_\mu^{(B)} + \hat{A}_\mu^{\gamma(B)} + \hat{Z}_{R\mu}^{(B)}. \end{aligned} \quad (\text{C.8})$$

The gauge couplings in (C.7) consist of

$$\begin{aligned} \bar{\Psi}_F \gamma^\mu (g_A \hat{V}_\mu) \Psi_F, & \quad \text{for } V = W, W_R, A^{\hat{4}}, \\ \bar{\Psi}_F \gamma^\mu (g_A \hat{V}_\mu^{(A)} + Q_X g_B \hat{V}_\mu^{(B)}) \Psi_F, & \quad \text{for } V = A^\gamma, Z, Z_R. \end{aligned} \quad (\text{C.9})$$

Each tower is decomposed to KK modes. For W , W_R and $A^{\hat{4}}$ bosons

$$\begin{aligned} \hat{W}_\mu^\pm &= \sum_n W_\mu^{\pm(n)}(x) \left\{ h_{W^{(n)}}^L \frac{T^{1L} \pm iT^{2L}}{\sqrt{2}} + h_{W^{(n)}}^R \frac{T^{1R} \pm iT^{2R}}{\sqrt{2}} + \hat{h}_{W^{(n)}} \frac{T^{\hat{1}} \pm iT^{\hat{2}}}{\sqrt{2}} \right\}, \\ \hat{W}_{R\mu}^\pm &= \sum_n W_{R\mu}^{\pm(n)}(x) \left\{ h_{W_R^{(n)}}^L \frac{T^{1L} \pm iT^{2L}}{\sqrt{2}} + h_{W_R^{(n)}}^R \frac{T^{1R} \pm iT^{2R}}{\sqrt{2}} + \hat{h}_{W_R^{(n)}} \frac{T^{\hat{1}} \pm iT^{\hat{2}}}{\sqrt{2}} \right\}, \\ \hat{A}_\mu^{\hat{4}} &= \sum_n A_\mu^{\hat{4}(n)}(x) h_{A^{\hat{4}(n)}} T^{\hat{4}}, \end{aligned} \quad (\text{C.10})$$

where $\hat{W}_\mu^\pm = (\hat{W}_\mu^1 \mp i\hat{W}_\mu^2)/\sqrt{2}$ etc., whereas for A^γ , Z and Z_R bosons

$$\begin{aligned} (\hat{A}_\mu^{\gamma(A)}, \hat{A}_\mu^{\gamma(B)}) &= \sum_n A_\mu^{\gamma(n)}(x) (h_{\gamma^{(n)}}^L T^{3L} + h_{\gamma^{(n)}}^R T^{3R}, h_{\gamma^{(n)}}^B), \\ (\hat{Z}_\mu^{(A)}, \hat{Z}_\mu^{(B)}) &= \sum_n Z_\mu^{(n)}(x) (h_{Z^{(n)}}^L T^{3L} + h_{Z^{(n)}}^R T^{3R} + \hat{h}_{Z^{(n)}} T^{\hat{3}}, h_{Z^{(n)}}^B), \\ (\hat{Z}_{R\mu}^{(A)}, \hat{Z}_{R\mu}^{(B)}) &= \sum_n Z_{R\mu}^{(n)}(x) (h_{Z_R^{(n)}}^L T^{3L} + h_{Z_R^{(n)}}^R T^{3R}, h_{Z_R^{(n)}}^B). \end{aligned} \quad (\text{C.11})$$

Here $n = 0, 1, 2, \dots$ $[1, 2, \dots]$ for A_μ^γ , W_μ and Z_μ [$W_{R\mu}$, $Z_{R\mu}$ and $A_\mu^{\hat{4}}$]. $A_\mu^{\gamma(0)}$, $W_\mu^{(0)}$ and $Z_\mu^{(0)}$ correspond to the photon, W and Z bosons, respectively.

C.2.1 Couplings to $\gamma^{(n)}$, $Z^{(n)}$, $Z_R^{(n)}$ and $A^{\hat{4}}$

Here we summarize the dark fermion couplings to the neutral vector bosons. It would be useful to collect the building blocks for the couplings. For KK fermions $\Psi_F^{(n)}$ and $\Psi_F^{(m)}$, we

have

$$\begin{aligned}
\bar{\Psi}_F^{(n)} T^{3L} \gamma^\mu \Psi_F^{(m)} &= \frac{kz^4}{2} f_{lL}^{(n)*} f_{lL}^{(m)} [\bar{F}_L^{+(n)} \gamma^\mu F_L^{+(m)} - \bar{F}_L^{0(n)} \gamma^\mu F_L^{0(m)}] + (F_L, f_{lL} \rightarrow F_R, f_{lR}), \\
\bar{\Psi}_F^{(n)} T^{3R} \gamma^\mu \Psi_F^{(m)} &= \frac{kz^4}{2} f_{rL}^{(n)*} f_{rL}^{(m)} [\bar{F}_L^{+(n)} \gamma^\mu F_{L,m}^{+(m)} - \bar{F}_L^{0(n)} \gamma^\mu F_L^{0(m)}] + (F_L, f_{rL} \rightarrow F_R, f_{rR}), \\
\bar{\Psi}_F^{(n)} T^{\hat{3}} \gamma^\mu \Psi_F^{(m)} &= \frac{kz^4}{2\sqrt{2}} i [f_{lL}^{(n)*} f_{rL}^{(m)} - f_{rL}^{(n)*} f_{lL}^{(m)}] [\bar{F}_L^{+(n)} \gamma^\mu F_L^{+(m)} - \bar{F}_L^{0(n)} \gamma^\mu F_L^{0(m)}] \\
&\quad + (F_L, f_{lL}, f_{rL} \rightarrow F_R, f_{lR}, f_{rR}), \\
\bar{\Psi}_F^{(n)} \gamma^\mu \Psi_F^{(m)} &= kz^4 [f_{lL}^{(n)*} f_{lL}^{(m)} + f_{rL}^{(n)*} f_{rL}^{(m)}] [\bar{F}_L^{+(n)} \gamma^\mu F_L^{+(m)} + \bar{F}_L^{0(n)} \gamma^\mu F_L^{0(m)}] \\
&\quad + (F_L, f_{lL}, f_{rL} \rightarrow F_R, f_{lR}, f_{rR}).
\end{aligned} \tag{C.12}$$

In the followings we summarize the couplings in the case of $n = m = 1$.

Electromagnetic photon $\gamma = \gamma^{(0)}$ For the photon $A_\mu^{\gamma(0)}$, wave functions are given by

$$h_{\gamma(0)}^L = h_{\gamma(0)}^R = \frac{1}{\sqrt{(1+s_\phi^2)L}} s_\phi, \quad h_{\gamma(0)}^B = \frac{1}{\sqrt{(1+s_\phi^2)L}} c_\phi, \tag{C.13}$$

where c_ϕ and s_ϕ given by

$$c_\phi \equiv \cos \phi = \frac{g_A}{\sqrt{g_A^2 + g_B^2}}, \quad s_\phi \equiv \sin \phi = \frac{g_B}{\sqrt{g_A^2 + g_B^2}}, \tag{C.14}$$

parameterize the mixing of A_M and B_M , and are related to the Weinberg angle θ_W by $\sin \phi = \tan \theta_W$. The couplings between dark fermions and the photon can be read from

$$\begin{aligned}
&\int_1^{z_L} dz \sqrt{G} e_l^\mu \bar{\Psi}_F^{(n)} [g_A A_\mu^{\gamma(0)} + Q_X g_B A_\mu^{\gamma(0)}] \gamma^\mu \Psi_F^{(m)} \\
&= e A_\mu^{\gamma(0)}(x) \int_1^{z_L} dz \left\{ \left[f_{lL}^{(n)*} f_{lL}^{(m)} + f_{rL}^{(n)*} f_{rL}^{(m)} \right] \right. \\
&\quad \times \left[(Q_X + \frac{1}{2}) \bar{F}_L^{+(n)} \gamma^\mu F_L^{+(n)} + (Q_X - \frac{1}{2}) \bar{F}_L^{0(n)} \gamma^\mu F_L^{0(n)} \right] \left. \right\} + (L \rightarrow R) \\
&= e A_\mu^{\gamma(0)}(x) \delta_{n,m} \left\{ (Q_X + \frac{1}{2}) \bar{F}^{+(n)} \gamma^\mu F^{+(n)} + (Q_X - \frac{1}{2}) \bar{F}^{0(n)} \gamma^\mu F^{0(n)} \right\},
\end{aligned} \tag{C.15}$$

where the orthonormality conditions (B.9) has been used. F^+ [F^0] has electric charge $Q_X + \frac{1}{2}$ [$Q_X - \frac{1}{2}$]. The Kaluza-Klein level for fermions is preserved.

KK photons Wave functions for the KK photons $\gamma^{(n)}$ ($n \geq 1$) are given by

$$\begin{pmatrix} h_{\gamma^{(n)}}^L \\ h_{\gamma^{(n)}}^B \end{pmatrix} = \frac{1}{\sqrt{1+s_\phi^2}} \frac{1}{\sqrt{r_{\gamma^{(n)}}}} \begin{pmatrix} s_\phi \\ c_\phi \end{pmatrix} C(z), \quad r_{\gamma^{(n)}} = \int_1^{z_L} \frac{dz}{kz} C(z)^2, \tag{C.16}$$

Table 8: The mass and left- and right-handed couplings to F^+ in (C.17) in the unit of electromagnetic coupling e of the first KK photon in the case of degenerate dark fermions with the parameters specified in Table 2.

n_F	z_L	$m_{\gamma^{(1)}} [\text{TeV}]$	$g_{F^+L}^{\gamma^{(1)}}$	$g_{F^+R}^{\gamma^{(1)}}$
3	10^8	2.42	0.19	4.16
	10^6	4.26	0.28	3.61
	10^5	5.92	0.38	3.31
	2×10^4	7.55	0.52	3.09
4	10^8	2.46	0.06	4.15
	10^6	4.32	0.11	3.59
	10^5	6.00	0.15	3.28
	3×10^4	7.19	0.17	3.10
	10^4	8.52	0.21	2.93
6	10^8	2.50	-0.06	4.14
	10^6	4.40	-0.05	3.58
	10^5	6.12	-0.04	3.26
	10^4	8.68	-0.03	2.90

where $C(z) = C(z; \lambda_{\gamma^{(n)}})$ and $\lambda_{\gamma^{(n)}}$ satisfy $C'(1; \lambda_{\gamma^{(n)}}) = 0$. Hence the couplings are given by

$$\begin{aligned}
& \sum_{c=+,0} \gamma_\mu^{(n)} [g_{F^cL}^{\gamma^{(n)}} \bar{F}_L^c \gamma^\mu F_L^c + g_{F^cR}^{\gamma^{(n)}} \bar{F}_R^c \gamma^\mu F_R^c] \\
&= \gamma_\mu^{(n)}(x) \left\{ (Q_X + \frac{1}{2}) \bar{F}_L^+ \gamma^\mu F_L^+ + (Q_X - \frac{1}{2}) \bar{F}_L^0 \gamma^\mu F_L^0 \right\} \\
&\quad \times \frac{e\sqrt{L}}{\sqrt{r_{\gamma^{(n)}}}} \int_1^{z_L} dz C(z) [|f_{lL}|^2 + |f_{rL}|^2] + (L \rightarrow R) . \tag{C.17}
\end{aligned}$$

Note that the couplings are left-right asymmetric, i.e., $g_{F\gamma^{(n)}}^L \neq g_{F\gamma^{(n)}}^R$ for $n \geq 1$. In Tables 8 and 9, $\gamma^{(1)} F^+ F^-$ couplings are tabulated.

Z boson Wave functions of Z tower are given by

$$\begin{aligned}
& \begin{pmatrix} h_{Z^{(n)}}^L \\ h_{Z^{(n)}}^R \\ \hat{h}_{Z^{(n)}} \\ (g_B/g_A) h_{Z^{(n)}}^B \end{pmatrix} = \frac{1}{\sqrt{1+s_\phi^2}} \frac{1}{\sqrt{r_{Z^{(n)}}}} \begin{pmatrix} \frac{c_\phi^2 + (1+s_\phi^2) \cos \theta_H}{\sqrt{2}} C(z) \\ \frac{c_\phi^2 - (1+s_\phi^2) \cos \theta_H}{\sqrt{2}} C(z) \\ -(1+s_\phi^2) \sin \theta_H \hat{S}(z) \\ -\sqrt{2} s_\phi^2 C(z) \end{pmatrix}, \\
& r_{Z^{(n)}} = \int_1^{z_L} \frac{dz}{kz} \left\{ c_\phi^2 C(z)^2 + (1+s_\phi^2) [\cos^2 \theta_H C(z)^2 + \sin^2 \theta_H \hat{S}(z)^2] \right\}, \tag{C.18}
\end{aligned}$$

Table 9: The left- and right-handed couplings to the light F_l^+ in (C.17) in the unit of electromagnetic coupling e of the first KK photon in the case of non-degenerate $(n_F^{\text{light}}, n_F^{\text{heavy}}) = (1, 3)$ dark fermions with the parameters specified in Table 3.

Δc_F	z_L	$g_{F_L^+}^{\gamma^{(1)}}$	$g_{F_R^+}^{\gamma^{(1)}}$
0.04	10^6	0.03	3.58
	10^5	0.08	3.27
	3×10^4	0.11	3.09
	10^4	0.16	2.92
0.06	10^6	0.01	3.58
	10^5	0.04	3.26
	3×10^4	0.08	3.09
	10^4	0.13	2.92

where $C(z) \equiv C(z; \lambda_{Z^{(n)}})$, $\hat{S}(z) \equiv \hat{S}(z; \lambda_{Z^{(n)}})$ and $\lambda_{Z^{(n)}}$ satisfy

$$2S(z; \lambda_{Z^{(n)}})C'(z; \lambda_{Z^{(n)}}) + (1 + s_\phi^2)\lambda_{Z^{(n)}} \sin^2 \theta_H = 0. \quad (\text{C.19})$$

The smallest positive root $\lambda_{Z^{(0)}}$ is related to the Z -boson mass by $m_Z = k \cdot \lambda_{Z^{(0)}}$. In terms of these the couplings of F to the $Z^{(n)}$ boson are given by

$$\begin{aligned}
\mathcal{L}_{4D} &\supset Z_\mu^{(n)} \sum_{c=+,-} [g_{F^c L}^{Z^{(n)}} \bar{F}_L^c \gamma^\mu F_L^c + g_{F^c R}^{Z^{(n)}} \bar{F}_R^c \gamma^\mu F_R^c] \\
&= \frac{g_w \sqrt{L}}{\sqrt{2} \cos \theta_W \sqrt{r_{Z^{(n)}}}} Z_\mu^{(n)} \sum_{c=+,0} \bar{F}_L^c \gamma^\mu F_L^c \int_1^{z_L} dz \left[I_3^{(c)} \left\{ C(z) [|f_{lL}|^2 + |f_{rL}|^2] \right. \right. \\
&\quad \left. \left. + \cos \theta_H C(z) [|f_{lL}|^2 - |f_{rL}|^2] - i \sin \theta_H \hat{S}(z) [f_{lL}^* f_{rL} - f_{rL}^* f_{lL}] \right\} \right. \\
&\quad \left. - (Q_X + I_3^{(c)}) \sin^2 \theta_W \cdot 2C(z) [|f_{lL}|^2 + |f_{rL}|^2] \right] + (L \rightarrow R), \quad (\text{C.20})
\end{aligned}$$

where $I_3^{(c)} = \frac{1}{2} [-\frac{1}{2}]$ for $c = + [0]$. We note that if the F obey the boundary condition $\eta_F = +1$ the $Z^{(n)}$ coupling to a fermion F^0 with $Q_{EM} = Q_X + I_3^{(i)} = 0$ is suppressed by $\sin^2(\theta_H/2)$, because $f_{lL} \propto \sin(\theta_H/2)$. We have summarized the $ZF\bar{F}$ couplings in Tables 10, 11 and 12, and the $Z^{(1)}F\bar{F}$ couplings in Tables 13 and 14.

Table 10: The left- and right-handed couplings in the unit of g_w of F to the Z boson in (C.20) with b.c. $\eta_F = +1$ in the case of degenerate dark fermions with the parameters specified in Table 2.

n_F	z_L	g_{F+L}^Z	g_{F+R}^Z	$g_{F^0L}^Z \times 10^4$	$g_{F^0R}^Z \times 10^4$
3	10^8	-0.260	-0.242	-40.1	-227
	10^6	-0.261	-0.257	-21.8	-69.6
	10^5	-0.262	-0.260	-19.7	-42.7
	2×10^4	-0.259	-0.258	-41.3	-58.4
4	10^8	-0.261	-0.244	-25.2	-204.9
	10^6	-0.263	-0.258	-11.4	-55.9
	10^5	-0.263	-0.261	-7.6	-27.7
	3×10^4	-0.263	-0.262	-6.7	-19.7
	10^4	-0.263	-0.262	-6.5	-15.4
6	10^8	-0.263	-0.246	-14.2	-186.0
	10^6	-0.263	-0.259	-5.8	-47.7
	10^5	-0.263	-0.262	-3.4	-21.9
	10^4	-0.264	-0.263	-2.1	-9.8

Table 11: The left- and right-handed couplings in the unit of g_w of F to the Z boson in (C.20) with b.c. $\eta_F = -1$ in the case of degenerate dark fermions with the parameters specified in Table 2.

n_F	z_L	g_{F+L}^Z	g_{F+R}^Z	$g_{F^0L}^Z$	$g_{F^0R}^Z$
4	10^8	0.304	0.287	-0.569	-0.552
	10^6	0.306	0.301	-0.569	-0.565
	10^4	0.306	0.305	-0.570	-0.569

Table 12: The left- and right-handed couplings in the unit of g_w of F to the Z boson in (C.20) with b.c. $\eta_F = +1$ in the case of non-degenerate $(n_F^{\text{light}}, n_F^{\text{heavy}}) = (1, 3)$ dark fermions with the parameters specified in Table 3.

Δc_F	z_L	g_{F+L}^Z	g_{F+R}^Z	$g_{F^0L}^Z \times 10^4$	$g_{F^0R}^Z \times 10^4$
0.04	10^6	-0.263	-0.259	-8.4	-52.2
	10^5	-0.263	-0.261	-5.9	-25.5
	3×10^4	-0.263	-0.262	-5.1	-17.8
	10^4	-0.263	-0.262	-5.0	-13.5
0.06	10^6	-0.263	-0.259	-7.2	-50.8
	10^5	-0.263	-0.261	-5.1	-24.6
	3×10^4	-0.263	-0.262	-4.5	-17.0
	10^4	-0.263	-0.263	-4.4	-12.8

Table 13: The left- and right-handed couplings in the unit of g_w of F to the first KK Z boson $Z^{(1)}$ in (C.20) with b.c. $\eta_F = +1$ in the case of degenerate dark fermions with the parameters specified in Table 2.

n_F	z_L	$m_{Z^{(1)}} [\text{TeV}]$	$g_{F+L}^{Z^{(1)}}$	$g_{F+R}^{Z^{(1)}}$	$g_{F^0L}^{Z^{(1)}}$	$g_{F^0R}^{Z^{(1)}}$
3	10^8	2.42	-0.02	-1.07	-0.04	-0.08
	10^6	4.25	-0.06	-0.95	-0.02	-0.02
	10^5	5.92	-0.09	-0.87	-0.01	-0.01
	2×10^4	7.54	-0.12	-0.81	-0.02	-0.00
4	10^8	2.45	0.00	-1.06	-0.02	-0.08
	10^6	4.32	-0.02	-0.94	-0.01	-0.02
	10^5	6.00	-0.03	-0.86	-0.01	-0.01
	10^4	8.52	-0.05	-0.77	-0.00	-0.00
6	10^8	2.50	0.02	-1.06	-0.01	-0.07
	10^6	4.40	0.02	-0.94	-0.00	-0.01
	10^5	6.13	0.01	-0.86	-0.00	-0.01
	10^4	8.68	0.01	-0.77	-0.00	-0.00

Table 14: The left- and right-handed couplings in the unit of g_w of F to the first KK Z boson $Z^{(1)}$ in (C.20) with b.c. $\eta_F = -1$ in the case of degenerate dark fermions with the parameters specified in Table 2.

n_F	z_L	$g_{F+L}^{Z^{(1)}}$	$g_{F+R}^{Z^{(1)}}$	$g_{F^0L}^{Z^{(1)}}$	$g_{F^0R}^{Z^{(1)}}$
4	10^8	0.00	1.25	-0.02	-2.39
	10^6	0.03	1.10	-0.06	-2.05
	10^5	0.04	1.00	-0.08	-1.87
	10^4	0.06	0.90	-0.12	-1.67

Z_R **boson** Wave functions of the Z_R -tower are given by

$$\begin{pmatrix} h_{Z_R^{(n)}}^L \\ h_{Z_R^{(n)}}^R \\ (g_B/g_A)h_{Z_R^{(n)}}^B \end{pmatrix} = \frac{1}{\sqrt{1 + (1 + 2t_\phi^2) \cos^2 \theta_H}} \frac{1}{\sqrt{r_{Z_R^{(n)}}}} \begin{pmatrix} \frac{1 - \cos \theta_H}{\sqrt{2}} \\ \frac{-1 - \cos \theta_H}{\sqrt{2}} \\ \sqrt{2} t_\phi^2 \cos \theta_H \end{pmatrix} C(z),$$

$$r_{Z_R^{(n)}} = \int_1^{z_L} \frac{dz}{kz} C(z)^2, \quad (\text{C.21})$$

where $C(z) = C(z; \lambda_{Z_R^{(n)}})$ and $\lambda_{Z_R^{(n)}}$ satisfy $C(1; \lambda_{Z_R^{(n)}}) = 0$. Hence the $Z_R^{(n)} \bar{F} F$ couplings are given by

$$\begin{aligned} \mathcal{L}_{4D} &\supset Z_{R\mu}^{(n)} \sum_{c=+,0} [g_{F^cL}^{Z_R^{(n)}} \bar{F}_L^c \gamma^\mu F_L^c + g_{F^cR}^{Z_R^{(n)}} \bar{F}_R^c \gamma^\mu F_R^c] \\ &= Z_{R\mu}^{(n)} \frac{g_w \sqrt{L}}{\sqrt{2} \sqrt{1 + \frac{\cos^2 \theta_H}{\cos 2\theta_W}} \sqrt{r_{Z_R^{(n)}}}} \sum_{c=+,0} \bar{F}_L^c \gamma^\mu F_L^c \int_1^{z_L} dz C(z) \\ &\quad \times \left[I_3^{(c)} \left\{ -\cos \theta_H [|f_{lL}|^2 + |f_{rL}|^2] + [|f_{lL}|^2 - |f_{rL}|^2] \right\} \right. \\ &\quad \left. + 2Q_X \frac{\sin^2 \theta_W}{\cos 2\theta_W} \cos \theta_H [|f_{lL}|^2 + |f_{rL}|^2] \right] + (L \rightarrow R). \end{aligned} \quad (\text{C.22})$$

We note that unlike the case of the Z boson the $Z_R F \bar{F}$ couplings, where F obeys the b.c. $\eta_F = +1$, are not suppressed even if $\theta_H \rightarrow 0$.

In Tables 15, 16 and 17, we have summarized the $Z_R \bar{F} F$ couplings.

Table 15: The left- and right-handed couplings in the unit of g_w of F to $Z_R^{(1)}$ in (C.22) with b.c. $\eta_F = +1$ in the case of degenerate dark fermions with the parameters specified in Table 2.

n_F	z_L	$m_{Z_R^{(1)}} [\text{TeV}]$	$g_{F^+L}^{Z_R^{(1)}}$	$g_{F^+R}^{Z_R^{(1)}}$	$g_{F^0L}^{Z_R^{(1)}}$	$g_{F^0R}^{Z_R^{(1)}}$
3	10^8	2.34	-0.09	-1.05	0.25	2.55
	10^6	4.06	-0.13	-0.90	0.34	2.23
	10^5	5.59	-0.16	-0.82	0.42	2.06
	2×10^4	7.05	-0.20	-0.77	0.51	1.93
4	10^8	2.37	-0.07	-1.05	0.18	2.54
	10^6	4.12	-0.10	-0.89	0.24	2.22
	10^5	5.70	-0.11	-0.82	0.29	2.04
	3×10^4	6.74	-0.12	-0.78	0.32	1.94
	10^4	7.92	-0.14	-0.73	0.35	1.84
6	10^8	2.42	-0.04	-1.05	0.12	2.54
	10^6	4.20	-0.06	-0.89	0.16	2.21
	10^5	5.78	-0.07	-0.81	0.18	2.03
	10^4	8.11	-0.08	-0.73	0.21	1.83

Table 16: The left- and right-handed couplings in the unit of g_w of F to $Z_R^{(1)}$ in (C.22) with b.c. $\eta_F = -1$ in the case of degenerate dark fermions with the parameters specified in Table 2.

n_F	z_L	$g_{F^+L}^{Z_R^{(1)}}$	$g_{F^+R}^{Z_R^{(1)}}$	$g_{F^0L}^{Z_R^{(1)}}$	$g_{F^0R}^{Z_R^{(1)}}$
4	10^8	0.05	0.80	0.07	0.69
	10^6	0.07	0.68	0.08	0.65
	10^5	0.08	0.62	0.09	0.61
	3×10^4	0.09	0.58	0.10	0.58
	10^4	0.11	0.55	0.11	0.55

Table 17: The left- and right-handed couplings in the unit of g_w of F to $Z_R^{(1)}$ in (C.22) with b.c. $\eta_F = +1$ in the case of non-degenerate $(n_F^{\text{light}}, n_F^{\text{heavy}}) = (1, 3)$ dark fermions with the parameters specified in Table 3.

Δc_F	z_L	$g_{F^+L}^{Z_R^{(1)}}$	$g_{F^+R}^{Z_R^{(1)}}$	$g_{F^0L}^{Z_R^{(1)}}$	$g_{F^0R}^{Z_R^{(1)}}$
0.04	10^6	-0.08	-0.89	0.20	2.22
	10^5	-0.10	-0.81	0.25	2.03
	3×10^4	-0.11	-0.77	0.28	1.93
	10^4	-0.13	-0.73	0.32	1.84
0.06	10^6	-0.07	-0.89	0.18	2.21
	10^5	-0.09	-0.81	0.23	2.03
	3×10^4	-0.10	-0.77	0.26	1.93
	10^4	-0.12	-0.73	0.30	1.83

A^4 **boson** Diagonal $\bar{F}^{(n)} F^{(n)} A_\mu^4$ couplings vanish, because one finds for the left-hand couplings

$$\begin{aligned}
& \bar{\Psi}_{FL}^{(m)} \gamma^\mu T^4 \Psi_{FL}^{(n)} \\
&= k z^4 \frac{1}{2\sqrt{2}} \bar{F}_L^{(m)} \gamma^\mu F_L^{(n)} (f_{lL}^{(m)*} f_{rL}^{(n)*}) \begin{pmatrix} & 1_2 \\ 1_2 & \end{pmatrix} \begin{pmatrix} f_{lL}^{(n)} \\ f_{rL}^{(n)} \end{pmatrix}, \\
&\propto \left\{ S_L(1, \lambda_m) C_L(z, \lambda_m) C_L(1, \lambda_n) S_L(z, \lambda_n) - (\lambda_m \leftrightarrow \lambda_n) \right\}, \tag{C.23}
\end{aligned}$$

and a similar relation for right-handed couplings.

C.2.2 Couplings to W and W_R bosons

The building-blocks for $W \bar{F} F$ and $W_R \bar{F} F$ couplings are

$$\begin{aligned}
\bar{\Psi}_F^{(n)} T^{+L} \gamma^\mu \Psi_F^{(m)} &= \frac{k z^4}{2} f_{lL}^{(n)*} f_{lL}^{(m)} [\bar{F}_L^{+(n)} \gamma^\mu F_L^{0(m)} - \bar{F}_L^{+(n)} \gamma^\mu F_L^{0(m)}] + (F_L, f_{lL} \rightarrow F_R, f_{lR}), \\
\bar{\Psi}_F^{(n)} T^{+R} \gamma^\mu \Psi_F^{(m)} &= \frac{k z^4}{2} f_{rL}^{(n)*} f_{rL}^{(m)} [\bar{F}_L^{+(n)} \gamma^\mu F_L^{0(m)} - \bar{F}_L^{+(n)} \gamma^\mu F_L^{0(m)}] + (F_L, f_{rL} \rightarrow F_R, f_{rR}), \\
\bar{\Psi}_F^{(n)} T^{\hat{+}} \gamma^\mu \Psi_F^{(m)} &= \frac{k z^4}{2} i [f_{lL}^{(n)*} f_{rL}^{(m)} - f_{rL}^{(n)*} f_{lL}^{(m)}] [\bar{F}_L^{+(n)} \gamma^\mu F_L^{0(m)} - \bar{F}_L^{+(n)} \gamma^\mu F_L^{0(m)}] \\
&\quad + (F_L, f_{lL}, f_{rL} \rightarrow F_R, f_{lR}, f_{rR}). \tag{C.24}
\end{aligned}$$

In the followings we summarize $W^- \bar{F}^{0(1)} F^{+(1)}$ and $W_R^- \bar{F}^{0(1)} F^{+(1)}$ ($m = n = 1$) couplings.

W boson Wave functions of the W -tower are

$$\begin{aligned} \begin{pmatrix} h_{W^{(n)}}^L \\ h_{W^{(n)}}^R \\ \hat{h}_{W^{(n)}} \end{pmatrix} &= \frac{1}{\sqrt{r_{W^{(n)}}}} \begin{pmatrix} \frac{1+\cos\theta_H}{\sqrt{2}} C(z) \\ \frac{1-\cos\theta_H}{\sqrt{2}} C(z) \\ -\sin\theta_H \hat{S}(z) \end{pmatrix}, \\ r_{W^{(n)}} &= \int_1^{z_L} \frac{dz}{kz} \left\{ (1 + \cos^2\theta_H) C(z)^2 + \sin^2\theta_H \hat{S}(z)^2 \right\}, \end{aligned} \quad (\text{C.25})$$

where $C(z) = C(z; \lambda_{W^{(n)}})$, $\hat{S}(z) = \hat{S}(z; \lambda_{W^{(n)}})$ and $\lambda_{W^{(n)}}$ satisfies

$$2S(z; \lambda_{W^{(n)}})C(1; \lambda_{W^{(n)}}) + \lambda_{W^{(n)}} \sin^2\theta_H = 0. \quad (\text{C.26})$$

$W^{(0)}$ is the W -boson whose mass is given by $m_W = k \cdot \lambda_{W^{(0)}}$. The couplings

$$\mathcal{L}_{4D} \supset W_\mu^{-(n)} \left[g_{FL}^{W^{(n)}} \bar{F}_L^0 \gamma^\mu F_L^+ + g_{FR}^{W^{(n)}} \bar{F}_R^0 \gamma^\mu F_R^+ \right] + (h.c.),$$

are given by

$$\begin{aligned} g_{FL}^{W^{(n)}} &= \frac{g_w}{2\sqrt{2}} \frac{\sqrt{L}}{\sqrt{r_{W^{(n)}}}} \int_1^{z_L} dz \left\{ C(z) [(1 + \cos\theta_H) |f_{lL}|^2 + (1 - \cos\theta_H) |f_{rL}|^2] \right. \\ &\quad \left. - \sin\theta_H \hat{S}(z) i[f_{lL}^* f_{rL} - f_{rL}^* f_{lL}] \right\}, \end{aligned} \quad (\text{C.27})$$

and $g_{FR}^{W^{(n)}}$ is obtained by replacements $f_{l(r)L} \rightarrow f_{l(r)R}$. We note that for the dark fermion obeying b.c. $\eta_F = +1$ these couplings are suppressed by $\sin^2(\theta_H/2)$, because $f_{lL} \propto \sin(\theta_H/2)$. The $WF\bar{F}$ and $W^{(1)}F\bar{F}$ couplings are summarized in Tables 18 and 19.

W_R boson Wave functions of W_R -tower are given by

$$\begin{aligned} \begin{pmatrix} h_{W_R^{(n)}}^L \\ h_{W_R^{(n)}}^R \end{pmatrix} &= \frac{1}{\sqrt{1 + \cos^2\theta_H}} \frac{1}{\sqrt{r_{W_R^{(n)}}}} \begin{pmatrix} \frac{-\cos\theta_H + 1}{\sqrt{2}} \\ \frac{-1 - \cos\theta_H}{\sqrt{2}} \end{pmatrix} C(z), \\ r_{W_R^{(n)}} &= \int_1^{z_L} \frac{dz}{kz} C(z)^2, \end{aligned} \quad (\text{C.28})$$

where $C(z) \equiv C(z; \lambda_{W_R^{(n)}})$ and $\lambda_{W_R^{(n)}}$ is defined by $C(1; \lambda_{W_R^{(n)}}) = 0$. In an analogous way to the W boson, we obtain the couplings

$$\begin{aligned} \mathcal{L}_{4D} &\supset W_{R\mu}^{-(n)} \left[g_{FL}^{W_R^{(n)}} \bar{F}_L^0 \gamma^\mu F_L^+ + g_{FR}^{W_R^{(n)}} \bar{F}_R^0 \gamma^\mu F_R^+ \right] + (h.c.), \\ g_{FL}^{W_R^{(n)}} &= \frac{g_w}{2\sqrt{2}} \frac{\sqrt{L}}{\sqrt{r_{W_R^{(n)}}} \sqrt{1 + \cos^2\theta_H}} \\ &\quad \times \int_1^{z_L} dz C(z) \left\{ (1 - \cos\theta_H) |f_{lL}|^2 + (-1 - \cos\theta_H) |f_{rL}|^2 \right\}, \end{aligned} \quad (\text{C.29})$$

and $g_{FR}^{W_R^{(n)}}$ is obtained by replacing $f_{l(r)L}$ with $f_{l(r)R}$. The $W_R^{(1)}F\bar{F}$ couplings are summarized in Tables 18 and 19.

Table 18: The left- and right-handed couplings $\bar{F}^0 F^+ V^-$ (in the unit of $g_w/\sqrt{2}$) of F to a charged vector boson V^- ($V = W, W^{(1)}$ and $W_R^{(1)}$) in (C.27) with b.c. $\eta_F = +1$ in the case of degenerate dark fermions with the parameters specified in Table 2.

n_F	z_L	g_{FL}^W $\times 10^3$	g_{FR}^W $\times 10^3$	$m_{W^{(1)}}$ [TeV]	$g_{FL}^{W^{(1)}}$ $\times 10^3$	$g_{FR}^{W^{(1)}}$ $\times 10^3$	$m_{W_R^{(1)}}$ [TeV]	$g_{FL}^{W_R^{(1)}}$	$g_{FR}^{W_R^{(1)}}$
3	10^8	7.0	39.8	2.42	61.9	136	2.34	-0.41	-3.11
	10^6	3.8	12.2	4.25	26.4	28.0	4.06	-0.57	-2.66
	2×10^4	7.2	10.2	7.54	31.5	7.8	7.05	-0.84	-2.28
4	10^8	4.4	35.9	2.45	40.2	132.2	2.37	-0.30	-3.10
	10^6	2.0	9.7	4.32	15.0	26.8	4.12	-0.41	-2.65
	10^4	1.1	2.7	8.52	6.1	3.8	7.92	-0.59	-2.18
6	10^8	2.5	32.6	2.50	23.4	127.3	2.42	-0.19	-3.10
	10^6	1.0	8.4	4.40	8.0	25.9	4.20	-0.26	-2.64
	10^4	0.4	1.7	8.68	2.3	3.6	8.07	-0.36	-2.16

Table 19: The left- and right-handed couplings $\bar{F}^0 F^+ V^-$ (in the unit of $g_w/\sqrt{2}$) of F to a charged vector boson V^- ($V = W, W^{(1)}$ and $W_R^{(1)}$) in (C.27) with b.c. $\eta_F = -1$ in the case of degenerate dark fermions with the parameters specified in Table 2.

n_F	z_L	g_{FL}^W	g_{FR}^W	$g_{FL}^{W^{(1)}}$	$g_{FR}^{W^{(1)}}$	$g_{FL}^{W_R^{(1)}}$	$g_{FR}^{W_R^{(1)}}$
4	10^8	0.997	0.966	0.04	4.15	-0.019	0.099
	10^6	0.998	0.991	0.10	3.59	-0.008	0.020
	10^4	0.999	0.998	0.21	2.93	-0.004	0.003

D VW^+W^- vector-boson couplings

In terms of the wave functions for the W boson and other neutral vector bosons $V = Z, Z_R, A^\gamma, A^{\hat{4}}$, one can read the VW^+W^- couplings from the relation

$$\begin{aligned} g_A \int_1^{z_L} \frac{dz}{kz} \text{tr} \partial_\mu \hat{V}_\nu [\hat{W}_\rho, \hat{W}_\sigma](x, z) \\ = \sum_{n,r,s} g_{V^{(n)}W^{+(r)}W^{-(s)}} (\partial_\mu V_\nu^{(n)}) W_\rho^{+(r)} W_\sigma^{-(s)}(x). \end{aligned} \quad (\text{D.1})$$

Hereafter we summarize the formulas for $V^{(n)}W^+W^-$ couplings. Numerically computed values of the VW^+W^- ($V = Z, Z^{(1)}, Z_R^{(1)}$ and $\gamma^{(1)}$) couplings are summarized in Table. 20. These couplings depend sensitively on z_L and θ_H , but very weakly on n_F , thanks to the universality relations in the model.[15, 16]

$\gamma^{(n)}W^+W^-$ coupling The $\gamma^{(n)}W^+W^-$ coupling is given by

$$g_{\gamma^{(n)}WW} = g_w \sqrt{L} \int_1^{z_L} \frac{dz}{kz} \left\{ h_{\gamma^{(n)}}^L \left[(h_W^L)^2 + \frac{(\hat{h}_W)^2}{2} \right] + h_{\gamma^{(n)}}^R \left[(h_W^R)^2 + \frac{(\hat{h}_W)^2}{2} \right] \right\}. \quad (\text{D.2})$$

In particular, for the photon $\gamma = \gamma^{(0)}$ we obtain

$$g_{\gamma WW} = e \quad (\text{electromagnetic coupling}), \quad (\text{D.3})$$

and for KK excited photons ($n \neq 0$) we have

$$g_{\gamma^{(n)}WW} = e \sqrt{L} \int_1^{z_L} \frac{dz}{kz} \frac{C(z, \lambda_{\gamma^{(n)}})}{\sqrt{r_{\gamma^{(n)}}}} [(h_W^L)^2 + (h_W^R)^2 + (\hat{h}_W)^2]. \quad (\text{D.4})$$

$Z^{(n)}W^+W^-$ coupling

$$\begin{aligned} g_{Z^{(n)}WW} = g_w \sqrt{L} \int_1^{z_L} \frac{dz}{kz} \left\{ h_{Z^{(n)}}^L \left[(h_W^L)^2 + \frac{(\hat{h}_W)^2}{2} \right] + h_{Z^{(n)}}^R \left[(h_W^R)^2 + \frac{(\hat{h}_W)^2}{2} \right] \right. \\ \left. + \hat{h}_{Z^{(n)}} (h_W^L + h_W^R) \hat{h}_W \right\}. \end{aligned} \quad (\text{D.5})$$

$Z_R^{(n)}W^+W^-$ coupling

$$g_{Z_R^{(n)}WW} = g_w \sqrt{L} \int_1^{z_L} \frac{dz}{kz} \left\{ h_{Z_R^{(n)}}^L \left[(h_W^L)^2 + \frac{(\hat{h}_W)^2}{2} \right] + h_{Z_R^{(n)}}^R \left[(h_W^R)^2 + \frac{(\hat{h}_W)^2}{2} \right] \right\}. \quad (\text{D.6})$$

We note that this coupling is suppressed by $\sin^2 \theta_H$ because

$$h_{Z_R}^L, h_W^R \propto \sin^2(\theta_H/2), \quad \hat{h}_W \propto \sin \theta_H.$$

Table 20: Triple vector-boson couplings VW^+W^- with $V = Z, Z^{(1)}, Z_R^{(1)}$ (D.5), (D.6) in unit of g_w and $\gamma^{(1)}W^+W^-$ in unit of the electric charge e .

n_F	z_L	g_{WWZ}	$g_{WWZ^{(1)}} \times 10^2$	$g_{WWZ_R^{(1)}} \times 10^2$	$g_{WW\gamma^{(1)}} \times 10^2$
4	10^8	0.811	1.506	0.391	-0.417
	10^6	0.861	0.459	0.114	-0.115
	10^5	0.870	0.225	0.055	-0.054
	10^4	0.874	0.105	0.025	-0.024

$A^{\hat{4}(n)}W^+W^-$ **coupling** $A^{\hat{4}(n)}W^{+(r)}W^{-(s)}$ coupling vanishes when $r = s$. In particular, for $r = s = 0$ we obtain

$$g_{A^{\hat{4}(n)}WW} = 0. \quad (\text{D.7})$$

$W_R^{+(n)}W^-Z$ **coupling**

$$g_{W_R^{(n)}WZ} = g_w \sqrt{L} \int_1^{z_L} \frac{dz}{kz} \left[h_{W_R^{(n)}}^L h_W^L h_Z^L + h_{W_R^{(n)}}^R h_W^R h_Z^R + \frac{1}{2} (h_{W_R^{(n)}}^L + h_{W_R^{(n)}}^R) \hat{h}_W \hat{h}_Z \right]. \quad (\text{D.8})$$

This coupling is suppressed by $\sin^2(\theta_H/2)$ because $h_{W_R^{(n)}}^L h_{W^{(n)}}^L, h_{W_R^{(n)}}^R h_{W^{(n)}}^R, \hat{h}_{W^{(n)}} \hat{h}_{Z^{(n)}} \propto \sin^2(\theta_H/2)$.

References

- [1] G. Aad *et al.* [ATLAS Collaboration], “Observation of a new particle in the search for the Standard Model Higgs boson with the ATLAS detector at the LHC”, *Phys. Lett. B* **716**, 1 (2012).
- [2] S. Chatrchyan *et al.* [CMS Collaboration], “Observation of a new boson at a mass of 125 GeV with the CMS experiment at the LHC”, *Phys. Lett. B* **716**, 30 (2012).
- [3] Y. Hosotani, “Dynamical Mass Generation by Compact Extra Dimensions”, *Phys. Lett. B* **126**, 309 (1983); “Dynamics of Nonintegrable Phases and Gauge Symmetry Breaking”, *Ann. Phys. (N.Y.)* **190**, 233 (1989).
- [4] A. T. Davies and A. McLachlan, “Gauge group breaking by Wilson loops”, *Phys. Lett. B* **200**, 305 (1988); “Congruency class effects in the Hosotani model”, *Nucl. Phys. B* **317**, 237 (1989).

- [5] H. Hatanaka, T. Inami and C.S. Lim, “*The gauge hierarchy problem and higher dimensional gauge theories*”, *Mod. Phys. Lett.* **A13**, 2601 (1998).
- [6] G. Burdman and Y. Nomura, “*Unification of Higgs and Gauge Fields in Five Dimensions*”, *Nucl. Phys.* **B656**, 3 (2003).
- [7] C. Csaki, C. Grojean and H. Murayama, “*Standard Model Higgs From Higher Dimensional Gauge Fields*”, *Phys. Rev.* **D67**, 085012 (2003).
- [8] C. S. Lim, “*The Higgs Particle and Higher-Dimensional Theories*”, *Prog. Theor. Exp. Phys.* **2014**, 02A101 (2014).
- [9] K. Agashe, R. Contino and A. Pomarol, “*The Minimal Composite Higgs Model*”, *Nucl. Phys.* **B719**, 165 (2005).
- [10] A. D. Medina, N. R. Shah and C. E. M. Wagner, “*Gauge-Higgs Unification and Radiative Electroweak Symmetry Breaking in Warped Extra Dimensions*”, *Phys. Rev.* **D76**, 095010 (2007).
- [11] Y. Hosotani, K. Oda, T. Ohnuma and Y. Sakamura, “*Dynamical Electroweak Symmetry Breaking in $SO(5) \times U(1)$ Gauge-Higgs Unification with Top and Bottom Quarks*”, *Phys. Rev.* **D78**, 096002 (2008); *Erratum-ibid.* **79**, 079902 (2009).
- [12] Y. Hosotani, S. Noda and N. Uekusa, “*The Electroweak gauge couplings in $SO(5) \times U(1)$ gauge-Higgs unification*”, *Prog. Theoret. Phys.* **123**, 757 (2010).
- [13] Y. Hosotani, M. Tanaka and N. Uekusa, “*H parity and the stable Higgs boson in the $SO(5) \times U(1)$ gauge-Higgs unification*”, *Phys. Rev.* **D82**, 115024 (2011).
- [14] Y. Hosotani, M. Tanaka, and N. Uekusa, “*Collider signatures of the $SO(5) \times U(1)$ gauge-Higgs unification*”, *Phys. Rev.* **D84**, 075014 (2011).
- [15] S. Funatsu, H. Hatanaka, Y. Hosotani, Y. Orikasa, and T. Shimotani, “*Novel universality and Higgs decay $H \rightarrow \gamma\gamma, gg$ in the $SO(5) \times U(1)$ gauge-Higgs unification*”, *Phys. Lett.* **B722**, 94 (2013).
- [16] S. Funatsu, H. Hatanaka, Y. Hosotani, Y. Orikasa and T. Shimotani, “*LHC signals of the $SO(5) \times U(1)$ gauge-Higgs unification*”, *Phys. Rev.* **D89**, 095019 (2014). [arXiv:1404.2748 [hep-ph]].
- [17] Y. Sakamura and Y. Hosotani, “*WWZ, WWH, and ZZH Couplings in the Dynamical Gauge-Higgs Unification in the Warped Spacetime*”, *Phys. Lett.* **B645**, 442 (2007).
- [18] Y. Hosotani and Y. Sakamura, “*Anomalous Higgs Couplings in the $SO(5) \times U(1)_{B-L}$ Gauge-Higgs Unification in Warped Spacetime*”, *Prog. Theoret. Phys.* **118**, 935 (2007).

- [19] G.F. Giudice, C. Grojean, A. Pomarol and R. Rattazzi, “*The Strongly-Interacting Light Higgs*”, *JHEP* **0706**, 045 (2007).
- [20] Y. Sakamura, “*Effective theories of gauge-Higgs unification models in warped space-time*”, *Phys. Rev. D* **76**, 065002 (2007).
- [21] Y. Hosotani and Y. Kobayashi, “*Yukawa Couplings and Effective Interactions in Gauge-Higgs Unification*”, *Phys. Lett. B* **674**, 192 (2009).
- [22] K. Hasegawa, N. Kurahashi, C. S. Lim and K. Tanabe, “*Anomalous Higgs Interactions in Gauge-Higgs Unification*”, *Phys. Rev. D* **87**, 016011 (2013).
- [23] N. Haba, Y. Sakamura and T. Yamashita, “*Weak boson scattering in Gauge-Higgs Unification*”, *JHEP* **0907**, 020 (2009).
- [24] Y. Adachi, C.S. Lim and N. Maru, “*Finite anomalous magnetic moment in the gauge-Higgs unification*”, *Phys. Rev. D* **76**, 075009 (2007); “*More on the Finiteness of Anomalous Magnetic Moment in the Gauge-Higgs Unification*”, *Phys. Rev. D* **79**, 075018 (2009).
- [25] M. Carena, A. D. Medina, B. Panes, N. R. Shah and C. E. M. Wagner, “*Collider Phenomenology of Gauge-Higgs Unification Scenarios in Warped Extra Dimensions*”, *Phys. Rev. D* **77**, 076003 (2008).
- [26] Y. Adachi, C.S. Lim and N. Maru, “*Neutron Electric Dipole Moment in the Gauge-Higgs Unification*”, *Phys. Rev. D* **80**, 055025 (2009).
- [27] K. Agashe, A. Azatov, T. Han, Y. Li, Z.G. Si, L. Zhu, “*LHC Signals for Coset Electroweak Gauge Bosons in Warped/Composite PGB Higgs Models*”, *Phys. Rev. D* **81**, 096002 (2010).
- [28] Y. Adachi, N. Kurahashi, C. S. Lim and N. Maru, “*Flavor Mixing in Gauge-Higgs Unification*”, *JHEP* **1011**, 150 (2010).
- [29] Y. Adachi, N. Kurahashi, N. Maru and K. Tanabe, “ *B^0 - \bar{B}^0 Mixing in Gauge-Higgs Unification*”, *Phys. Rev. D* **85**, 096001 (2012).
- [30] N. Haba, K. Kaneta and S. Tsuno, “*QCD parity violation at LHC in warped extra dimension*”, *Phys. Rev. D* **87**, 095002 (2013).
- [31] N. Maru and N. Okada, “*Diphoton decay excess and 125 GeV Higgs boson in gauge-Higgs unification*”, *Phys. Rev. D* **87**, 095019 (2013); “ *$H \rightarrow Z\gamma$ in gauge-Higgs unification*”, *Phys. Rev. D* **88**, 037701 (2013); “*125 GeV Higgs Boson and TeV Scale Colored Fermions in Gauge-Higgs Unification*”, arXiv:1310.3348 [hep-ph].

- [32] M. Kakizaki, S. Kanemura, H. Taniguchi and T. Yamashita, “*Higgs sector as a Probe of Supersymmetric Grand Unification with the Hosotani Mechanism*”, *Phys. Rev. D* **89**, 075013 (2014). [arXiv:1312.7575 [hep-ph]].
- [33] Y. Adachi, N. Kurahashi and N. Maru, “ $\mu \rightarrow 3e$ and $\mu \rightarrow e$ Conversion in Gauge-Higgs Unification”, arXiv:1404.4281 [hep-ph].
- [34] E. W. Kolb and M. S. Turner, “*The Early Universe*”, *Front. Phys.* **69**, 1 (1990).
- [35] G. Jungman, M. Kamionkowski and K. Griest, “*Supersymmetric dark matter*”, *Phys. Rep.* **267**, 195 (1996).
- [36] J. Ellis, A. Ferstl and K.A. Olive, “*Re-evaluation of the elastic scattering of supersymmetric dark matter*”, *Phys. Lett. B* **481**, 304 (2000).
- [37] G. Servant and T. M. P. Tait, “*Is the lightest Kaluza-Klein particle a viable dark matter candidate?*”, *Nucl. Phys. B* **650**, 391 (2003).
- [38] M. Kakizaki, S. Matsumoto, Y. Sato and M. Senami, “*Relic abundance of LKP dark matter in UED model including effects of second KK resonances*”, *Nucl. Phys. B* **735**, 84 (2006).
- [39] M. Kakizaki, S. Matsumoto and M. Senami, “*Relic abundance of dark matter in the minimal universal extra dimension model*”, *Phys. Rev. D* **74**, 023504 (2006).
- [40] G. Belanger, M. Kakizaki, and A. Pukhov, “*Dark matter in UED: The Role of the second KK level*”, *JCAP* **1102**, 009 (2011).
- [41] S. C. Park and J. Shu, “*Split Universal Extra Dimensions and Dark Matter*”, *Phys. Rev. D* **79**, 091702 (2009).
- [42] C. -R. Chen, M. M. Nojiri, S. C. Park, J. Shu and M. Takeuchi, “*Dark matter and collider phenomenology of split-UED*”, *JHEP* **0909**, 078 (2009).
- [43] M. Perelstein and A. Spray, “*Indirect Detection of Little Higgs Dark Matter*”, *Phys. Rev. D* **75**, 083519 (2007).
- [44] D. Hooper and G. Zaharijas, “*Distinguishing Supersymmetry From Universal Extra Dimensions or Little Higgs Models With Dark Matter Experiments*”, *Phys. Rev. D* **75**, 035010 (2007); A. Birkedal, A. Noble, M. Perelstein and A. Spray, “*Little Higgs dark matter*”, *Phys. Rev. D* **74**, 035002 (2006).
- [45] J. L. Diaz-Cruz, “*Holographic dark matter and Higgs*”, *Phys. Rev. Lett.* **100**, 221802 (2008).
- [46] M. Y. Khlopov and C. Kouvaris, “*Composite dark matter from a model with composite Higgs boson*”, *Phys. Rev. D* **78**, 065040 (2008).

- [47] M. Chala, “ $h \rightarrow \gamma\gamma$ excess and Dark Matter from Composite Higgs Models”, *JHEP* **1301**, 122 (2013).
- [48] J. Preskill, M. B. Wise and F. Wilczek, “Cosmology of the Invisible Axion”, *Phys. Lett.* **B120**, 127 (1983).
- [49] L. F. Abbott and P. Sikivie, “A Cosmological Bound on the Invisible Axion”, *Phys. Lett.* **B120**, 133 (1983).
- [50] M. Dine and W. Fischler, “The Not So Harmless Axion”, *Phys. Lett.* **B120**, 137 (1983).
- [51] L. D. Duffy and K. van Bibber, “Axions as Dark Matter Particles”, *New. J. Phys.* **11**, 105008 (2009).
- [52] L. Covi, J. E. Kim and L. Roszkowski, “Axinos as cold dark matter”, *Phys. Rev. Lett.* **82**, 4180 (1999).
- [53] V. Silveira and A. Zee, “Scalar Phantoms”, *Phys. Lett.* **B161**, 136 (1985).
- [54] H. Davoudiasl, R. Kitano, T. Li and H. Murayama, “The New minimal standard model”, *Phys. Lett.* **B609**, 117 (2005).
- [55] B. Patt and F. Wilczek, “Higgs-field portal into hidden sectors”, hep-ph/0605188.
- [56] S. Baek, P. Ko and W. -I. Park, “Invisible Higgs Decay Width vs. Dark Matter Direct Detection Cross Section in Higgs Portal Dark Matter Models”, arXiv:1405.3530 [hep-ph].
- [57] H. Okada and Y. Orikasa, “X-ray line in Radiative Neutrino Model with Global $U(1)$ Symmetry”, arXiv:1407.2543 [hep-ph].
- [58] K. R. Dienes and B. Thomas, “Dynamical Dark Matter: I. Theoretical Overview”, *Phys. Rev.* **D85**, 083523 (2012); “Dynamical Dark Matter: II. An Explicit Model”, *Phys. Rev.* **D85**, 083524 (2012).
- [59] G. Panico, E. Ponton, J. Santiago and M. Serone, “Dark Matter and Electroweak Symmetry Breaking in Models with Warped Extra Dimensions”, *Phys. Rev.* **D77**, 115012 (2008).
- [60] M. Carena, A. D. Medina, N. R. Shah and C. E. M. Wagner, “Gauge-Higgs Unification, Neutrino Masses and Dark Matter in Warped Extra Dimensions”, *Phys. Rev.* **D79**, 096010 (2009).
- [61] Y. Hosotani, P. Ko and M. Tanaka, “Stable Higgs Bosons as Cold Dark Matter”, *Phys. Lett.* **B680**, 179 (2009).
- [62] N. Haba, S. Matsumoto, N. Okada and T. Yamashita, “Gauge-Higgs Dark Matter”, *JHEP* **1003**, 064 (2010).

- [63] E. Aprile *et al.* [XENON100 Collaboration], “Dark Matter Results from 225 Live Days of XENON100 Data”, *Phys. Rev. Lett.* **109**, 181301 (2012).
- [64] D.S. Akerib *et al.* [LUX Collaboration], “First results from the LUX dark matter experiment at the Sanford Underground Research Facility”, *Phys. Rev. Lett.* **112**, 091303 (2014).
- [65] N. Haba, M. Harada, Y. Hosotani and Y. Kawamura, “Dynamical rearrangement of gauge symmetry on the orbifold S^1/Z_2 ”, *Nucl. Phys.* **B657**, 169 (2003); *Erratum-ibid.* **669**, 381 (2003).
- [66] N. Haba, Y. Hosotani and Y. Kawamura, “Classification and dynamics of equivalence classes in $SU(N)$ gauge theory on the orbifold S^1/Z_2 ”, *Prog. Theoret. Phys.* **111**, 265 (2004).
- [67] K. Yamamoto “The formulation of gauge-Higgs unification with dynamical boundary conditions”, *Nucl. Phys.* **B883**, 45 (2014). [arXiv:1401.0466 [hep-th]].
- [68] G. Cossu, H. Hatanaka, Y. Hosotani and J. -I. Noaki, “Polyakov loops and the Hosotani mechanism on the lattice”, *Phys. Rev.* **D89**, 094509 (2014). [arXiv:1309.4198 [hep-lat]].
- [69] B. Gripaios, A. Pomarol, F. Riva and J. Serra, “Beyond the Minimal Composite Higgs Model”, *JHEP* **0904**, 070 (2009).
- [70] Y. Matsumoto and Y. Sakamura, “6D gauge-Higgs unification on T^2/Z_N with custodial symmetry”, arXiv:1407.0133 [hep-ph].
- [71] K. Griest and D. Seckel, “Three exceptions in the calculation of relic abundances”, *Phys. Rev.* **D43**, 3191 (1991).
- [72] H. -C. Cheng, K. T. Matchev and M. Schmaltz, “Radiative corrections to Kaluza-Klein masses”, *Phys. Rev.* **D66**, 036005 (2002).
- [73] L. Randall and M. D. Schwartz, “Quantum field theory and unification in AdS_5 ”, *JHEP* **0111**, 003 (2001); “Unification and the hierarchy from AdS_5 ”, *Phys. Rev. Lett.* **88**, 081801 (2002).
- [74] M. Srednicki, R. Watkins and K. A. Olive, “Calculations of Relic Densities in the Early Universe”, *Nucl. Phys.* **B310**, 693 (1988).
- [75] J. Beringer *et al.* [Particle Data Group Collaboration], “Review of Particle Physics (RPP)”, *Phys. Rev. D* **86**, 010001 (2012).
- [76] P. A. R. Ade *et al.* [Planck Collaboration], “Planck 2013 results. XVI. Cosmological parameters”, arXiv:1303.5076 [astro-ph.CO].

- [77] M. E. Peskin and T. Takeuchi, “A new constraint on a strongly interacting Higgs sector”, *Phys. Rev. Lett.* **65**, 964 (1990); “Estimation of oblique electroweak corrections”, *Phys. Rev. D* **46**, 381 (1992).
- [78] W. D. Goldberger and M. B. Wise, “Modulus stabilization with bulk fields”, *Phys. Rev. Lett.* **83**, 4922 (1999).
- [79] P. Creminelli, A. Nicolis and R. Rattazzi, “Holography and the electroweak phase transition”, *JHEP* **0203**, 051 (2002).
- [80] M.W. Goodman and E. Witten, “Detectability of certain dark-matter candidates”, *Phys. Rev. D* **31**, 3059 (1986).
- [81] S. Dürr *et al.*, “Sigma term and strangeness content of octet baryons”, *Phys. Rev. D* **85**, 014509 (2012);
G. S. Bali *et al.*, [QCDSF Collaboration], “The strange and light quark contributions to the nucleon mass from Lattice QCD”, *Phys. Rev. D* **85**, 054502 (2012);
S. Dinter *et al.*, “Sigma terms and strangeness content of the nucleon with $N_f = 2 + 1 + 1$ twisted mass fermions”, *JHEP* **08**, 037 (2012);
A. Semke, M. F. M. Lutz, “Strangeness in the baryon ground states”, *Phys. Lett. B* **717**, 242 (2012);
M. Engelhardt, “Strange quark contributions to nucleon mass and spin from lattice QCD”, *Phys. Rev. D* **86**, 114510 (2012);
H. Ohki *et al.*, [JLQCD Collaboration], “Nucleon strange quark content from $N_f = 2 + 1$ lattice QCD with exact chiral symmetry”, *Phys. Rev. D* **87**, 034509 (2013);
P. E. Shanahan, A. W. Thomas, and R. D. Young, “Sigma terms from an $SU(3)$ chiral extrapolation”, *Phys. Rev. D* **87**, 074503 (2013);
P. Junnarkar, A. Walker-Loud “The Scalar Strange Content of the Nucleon from Lattice QCD”, *Phys. Rev. D* **87**, 114510 (2013);
M. Gong *et al.*, “Strangeness and charmness content of nucleon from overlap fermions on 2+1-flavor domain-wall fermion configurations”, *Phys. Rev. D* **88**, 014503 (2013);
W. Freeman, D. Toussaint, [MILC Collaboration], “The intrinsic strangeness and charm of the nucleon using improved staggered fermions”, *Phys. Rev. D* **88**, 054503 (2013).